Published for SISSA by Springer

Received: April 4, 2019
Revised: August 1, 2019
Accepted: August 6, 2019
Published: August 26, 2019

One-loop angularity distributions with recoil using Soft-Collinear Effective Theory

Ankita Budhraja,[a] Ambar Jain[a] and Massimiliano Procura[b,c]

[a] *Indian Institute of Science Education and Research, Bhopal Bypass Road, Bhauri, Bhopal 462 066, Madhya Pradesh, India*

[b] *Fakultät für Physik, Universität Wien, Boltzmanngasse 5, 1090 Wien, Austria*

[c] *Theoretical Physics Department, CERN, 1 Esplanade des Particules, Geneva 23, Switzerland*

E-mail: ankitab@iiserb.ac.in, ambarj@iiserb.ac.in, mprocura@univie.ac.at

Abstract: Angularities are event shapes whose sensitivity to the splitting angle of a collinear emission is controlled by a continuous parameter b, with $-1 < b < \infty$. When measured with respect to the thrust axis, this class of QCD observables includes thrust ($b = 1$) and jet broadening ($b = 0$), the former being insensitive to the recoil of soft against collinear radiation, while the latter being maximally sensitive to it. Presently available analytic results for angularity distributions with $b \neq 0$ can be applied only close to the thrust limit since recoil effects have so far been neglected. As a first step to establish a comprehensive theoretical framework based on Soft-Collinear Effective Theory valid for all recoil-sensitive angularities, we compute for the first time angularity distributions at one-loop order in α_s for *all values of* b taking into account recoil effects. In the differential cross section, these amount to novel sub-leading singular contributions and/or power corrections, where the former are characterized by fractional powers of the angularity and contribute appreciably close to the peak region, also for $b \gtrsim 0.5$. Our calculations are checked against various limits known in the literature and agree with the numerical output of the Event2 generator.

Keywords: Jets, NLO Computations

ArXiv ePrint: 1903.11087

Open Access, © The Authors.
Article funded by SCOAP[3].

https://doi.org/10.1007/JHEP08(2019)144

JHEP08(2019)144

Contents

1 Introduction **1**

2 Factorization theorems for angularities with respect to the thrust axis **5**

3 Angularity jet function at one loop **10**
- 3.1 Angularity jet function at one-loop for $b > 0$ 10
- 3.2 Angularity jet function at one-loop for $b < 0$ 13
- 3.3 Jet broadening limit of the one-loop jet function 14

4 Angularity soft function at one loop **15**
- 4.1 Soft function calculation for $b > 0$ 15
- 4.2 Soft function calculation for $b < 0$ 17
- 4.3 Jet broadening limit of the one-loop soft function 18
  - 4.3.1 Limit $b \to 0^+$ 19
  - 4.3.2 Limit $b \to 0^-$ 20

5 One-loop angularity distributions from broadening-like factorization **20**
- 5.1 One-loop cross section for $b > 0$ 20
  - 5.1.1 Small-τ limit 22
  - 5.1.2 Small-b and the jet broadening limit 23
- 5.2 One-loop cross section for $b < 0$ 24
  - 5.2.1 Small-τ limit 26
  - 5.2.2 Small-b and the jet broadening limit 26

6 Numerical analysis and comparison against Event2 **27**

7 Conclusions **29**

A Plus distributions and their identities **31**
- A.1 Plus distributions over scalar domains 31
- A.2 Plus distributions over vector domains 32

B Evaluation of the one-loop jet function **33**
- B.1 Jet diagram (a) 33
- B.2 Jet diagram (b) 34
  - B.2.1 Positive-b angularities 34
  - B.2.2 Negative-b angularities 35
- B.3 Zero-bin contribution 35

C Evaluation of the one-loop soft function **36**

JHEP08(2019)144

D Evaluation of the soft convolution integral **36**
D.1 Soft convolution integral $\mathrm{I}_s^{(+)}(\tau_R)$ 37
D.2 Soft convolution integral $\mathrm{I}_s^{(-)}(\tau_R)$ 38

E Expansion of the constraint equations in various limits **38**
E.1 Solution to the constraint equation in r ($b > 0$) 38
E.1.1 Small-τ expansion for r 38
E.1.2 Small-b expansion for r 39
E.2 Solution to the constraint equation in s ($b < 0$) 40
E.2.1 Small-τ expansion for s 40
E.2.2 Small-b expansion for s 40

1 Introduction

Event shapes describe geometrical properties of the energy-momentum flow in QCD events and probe strong interactions at various energy scales. They were among the first observables introduced to test QCD and have been used over the years for tuning parton showers and non-perturbative components of Monte Carlo event generators as well as to gain insight into hadronization effects in QCD (see e.g. [1] and references therein). Moreover, the comparison between high-precision e^+e^- collider data against fixed-order and resummed event shape calculations has provided accurate determinations of the strong coupling α_s, as in [2–6]. More recently, event shape studies have also been extended to applications at hadron colliders (see e.g. [7, 8]), and more exclusive, non-global event shape and jet shape measurements have acquired an important role in jet substructure studies (see e.g. [9–12]).

In this paper we focus on a specific class of global e^+e^- event shapes, called angularities, which are defined as [13]

$$\tau_b = \frac{1}{Q} \sum_{i \in X} |p_{\perp i}| \, e^{-b|\eta_i|} \,, \tag{1.1}$$

where Q is the center-of-mass energy.[1] Here the sum runs over all final-state particles i, with $p_{\perp i}$ and η_i denoting transverse momentum and pseudo-rapidity, respectively, of the ith particle with respect to an appropriately chosen axis. In available data analyses [17] this is identified with the thrust axis [18, 19], which is defined by the unit vector $\hat{t}$ that maximises the ratio $\sum_i |\vec{p}_i \cdot \hat{t}| / \sum_i |\vec{p}_i|$.

For any given kinematic configuration, eq. (1.1) defines a one-parameter family of infrared and collinear safe observables for any real number b in the interval $-1 < b < \infty$.

[1] In the most commonly used notation, the angularity exponent b is replaced by $1 - a$ [13–16]. However, eq. (1.1) is more convenient for our study, where a key role is played by the jet broadening limit $b \to 0$.

JHEP08(2019)144

Angularities are a generalization of the classic QCD observables thrust and jet broadening, which are given by the special cases[2]

$$\text{Thrust}: \quad b = 1, \qquad \tau_1 = \frac{1}{Q} \sum_{i \in X} |p_{\perp i}|\, e^{-|\eta_i|}\,, \tag{1.2}$$

$$\text{Broadening}: \quad b = 0, \qquad \tau_0 = \frac{1}{Q} \sum_{i \in X} |p_{\perp i}|\,. \tag{1.3}$$

The possibility to tune the parameter b exposes us to a wealth of information which is not accessible when looking at a single event shape such as thrust or broadening. Indeed, a continuous change in the angularity exponent leads to a smooth variation of the sensitivity of τ_b to the splitting angle of a collinear emission. Varying b affects the transverse size of the jets that dominate each region of the τ_b-distribution, changes the proportion of two-jet-like and three-or-more-jet-like events in the peak region as well as non-perturbative corrections, as discussed in detail in ref. [22].

For angularities with $b \gtrsim 1$, the direction of the thrust axis is insensitive to recoil by soft radiation, but as $b \to 0$, this effect cannot be ignored [23]. One possibility to deal with this is to choose a recoil-insensitive axis [24].[3] In this paper, instead, we stick to the traditional thrust axis for the following reasons. First of all, the available analytic expressions for angularity distributions with respect to the thrust axis (with the exception of jet broadening) have been applied only for $b \gtrsim 0.5$ because of neglected recoil effects. Here we derive novel complementary results valid also for $b < 0.5$, thereby opening up the possibility of comparing against existing LEP data [17] to improve the extraction of the strong coupling from angularities, by extending the work of ref. [22]. Secondly, we aim to establish a novel general framework based on factorization for recoil-sensitive angularities with respect to the thrust axis, and this paper is a first step in this direction. Here we focus on fixed-order predictions derived in the framework of Soft-Collinear Effective Theory (SCET) [27–31] for recoil-sensitive angularities, which allows us to illustrate interesting features of the interplay between collinear radiation and soft radiation in shaping up the τ_b-distribution when we continuously vary b *over its whole range*. In a companion paper [32], we will address the resummation of logarithmically enhanced terms and the validation of the logarithmic structure of recoil-sensitive angularity cross sections at $\mathcal{O}(\alpha_s^2)$ as predicted by a SCET factorization formula.

For $\tau \ll 1$, it is known that these angularity cross sections for $b \gtrsim 0.5$ and $b = 0$ can be expressed in a factorized form in terms of a hard function multiplying convolutions of jet functions with a soft function, each encoding physics at a single dynamical scale (hard, collinear and soft, respectively), thereby facilitating the resummation of large logarithmic terms. Calculations of these angularity distributions with respect to the thrust axis were carried out at NLL accuracy in refs. [13, 15, 33–35]. Recently these observables have been analyzed up to NNLL including NNLO corrections [22] within SCET for the

[2] The conventional definition of total jet broadening [20, 21] amounts to $\tau_0/2$.

[3] We refer to [25, 26] for recent studies of angularity distributions with respect to the winner-take-all axis up to next-to-next-to-leading logarithmic (NNLL) accuracy with next-to-leading fixed-order (NLO) corrections.

JHEP08(2019)144

purpose of a precision determination of $\alpha_s(m_Z)$ from LEP data, thereby providing important complementary information to similar analyses of event shapes like thrust [2, 4] and C-parameter [36]. NNLL+NLO accuracy for angularities has also been reached using the semi-numerical method ARES [37] in [26], while the NNLL resummation of jet broadening in the SCET framework was achieved in [38].

By varying the angularity exponent b, the components of the momenta carried by the soft degrees of freedom in SCET can either be suppressed or not, compared to the collinear modes, as in the case of thrust and broadening, respectively. If one neglects masses of both hadrons[4] and quarks, the soft and collinear modes, in the light-cone coordinates, satisfy the condition

$$p^+ p^- \sim p_\perp^2 \,, \tag{1.4}$$

together with the additional constraint $|p_\perp| \, e^{-b|\eta|} \sim \tau_b$ imposed by the angularity measurement. For the left ($\bar{n}$-collinear) and right (n-collinear) hemispheres defined by the plane orthogonal to $\hat{t}$, this constraint amounts to

$$\begin{aligned} \text{Right hemisphere } (p^+ < p^-): \quad & |p_\perp| \left(\frac{p^+}{p^-}\right)^{\frac{b}{2}} = (p^+)^{\frac{1+b}{2}} (p^-)^{\frac{1-b}{2}} \sim \tau_b \,, \\ \text{Left hemisphere } (p^+ > p^-): \quad & |p_\perp| \left(\frac{p^-}{p^+}\right)^{\frac{b}{2}} = (p^+)^{\frac{1-b}{2}} (p^-)^{\frac{1+b}{2}} \sim \tau_b \,. \end{aligned} \tag{1.5}$$

In our calculations, we will refer to the angularities measured on the right and left hemisphere as τ_R and τ_L, respectively. The event-wide angularity is obtained by summing over the two hemispheres, $\tau_b = \tau_L + \tau_R$.

In the expressions above, the momentum p^μ is decomposed into light-cone components as

$$p^\mu = (p^+, p^-, p_\perp^\mu) = \frac{n^\mu}{2} p^- + \frac{\bar{n}^\mu}{2} p^+ + p_\perp^\mu; \quad p^+ = n \cdot p \,, \quad p^- = \bar{n} \cdot p \,, \tag{1.6}$$

with $n^\mu = (1,0,0,1)$, $\bar{n}^\mu = (1,0,0,-1)$ and $n \cdot \bar{n} = 2$, where we have assumed that the thrust axis is along the $\hat{z}$ axis ($\hat{n} = \hat{t}$). If we define the power counting parameter λ as

$$\lambda^{1+b} \sim \tau_b \,, \tag{1.7}$$

then the momenta corresponding to collinear and soft radiation obeying eqs. (1.4) and (1.5) have the following parametric scaling in λ,

$$p_n^\mu \sim Q(\lambda^2, 1, \lambda), \quad p_{\bar{n}}^\mu \sim Q(1, \lambda^2, \lambda), \quad p_s^\mu \sim Q(\lambda^{1+b}, \lambda^{1+b}, \lambda^{1+b}) \,. \tag{1.8}$$

For $b = 1$ ($b = 0$), namely in the thrust (broadening) case, p_s^μ has so-called ultrasoft (soft) scaling. The relative momentum scalings determined by the angularity exponent b controls the separation of the mass hyperbolae for soft and collinear modes, as illustrated in Figure 1. For angularities with $b < 0$ ($b > 0$), the soft mode lies on a heavier (lighter) mass hyperbola compared to the collinear modes.[5] For values of b near 0, the soft and collinear modes have similar scalings and recoil effects are particularly important.

[4] Hadron masses will be relevant for calculating non-perturbative power corrections to the event-shape distributions [39, 40], which is beyond the scope of this work.

[5] For simplicity, we will keep the name "soft" for both cases.

JHEP08(2019)144

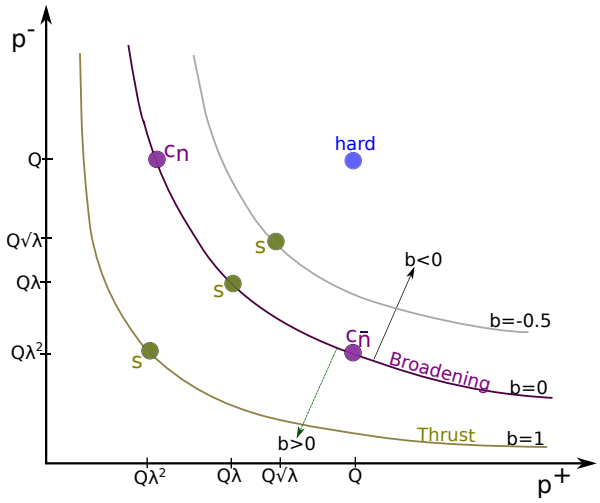

Figure 1. Invariant mass-hyperbolae and momentum scaling of collinear (c_n, $c_{\bar{n}}$) and soft (s) degrees of freedom for angularities with different exponents b. The power counting parameter λ is defined as $\lambda^{1+b} \sim \tau_b$.

If soft and collinear modes have relative scalings such that $p_c^2 \gg p_s^2$, which happens for $b \gtrsim 1$, then jet and soft sectors can be factorized on the basis of their invariant mass scales using the SCET_I framework, according to a *thrust-like* factorization theorem as in [15]. On the other hand, when the soft and collinear modes have similar invariant masses, $p_s^2 \sim p_c^2$, as is realized close to the jet broadening limit, the appropriate effective theory is SCET_II, which accounts for the recoil effects of soft against collinear radiation via convolutions in the transverse momenta carried by jet and soft functions, and enables the resummation of rapidity logarithms [34, 41] corresponding to rapidity divergences. Eq. (1.8) exhibits the fact that there is a continuous scaling of modes connecting these two regimes.

The main content of this paper can be summarized as follows. Starting from a SCET_II factorization formula that can be derived in full analogy with the one for jet broadening in ref. [34], we derive analytic expressions for the angularity distributions at one-loop for both positive and negative values of b and explicitly show their continuous behavior as $b \to 0$. We demonstrate that our cross section for $b > 0$ reduces to the known result from thrust-like factorization as b approaches 1 augmented by recoil effects which we are able to compute. In the differential angularity distributions with $0.5 < b < 1$, recoil effects amount to a sub-leading singular term and power corrections. The former is given by an integrable fractional power of τ_b whose numerical contribution at one-loop suggests that its all-order resummation might play an important role in precision calculations. Our analytic expressions for the angularity cross sections with $b < 0$ are the first derived within a SCET-based approach.[6] For both positive and negative values of b, we show how to recover the known results for the jet broadening distribution as well as the broadening jet and soft functions as $b \to 0$. Finally, we successfully compare our analytical expressions for $b \leq 0.5$ against Event2 and find that including sub-leading terms from our calculations can significantly improve the agreement with Event2 for the accessible range of values of τ.

[6]For an analysis based on the `ARES` method, we refer to [26].

JHEP08(2019)144

The authors of ref. [24] succeeded in defining a universal factorization framework for angularities measured with respect to a recoil-insensitive axis, like the winner-take-all or the broadening axis. This choice greatly simplifies the form of the factorization theorem by avoiding transverse momentum convolutions. Rapidity logarithms are important only for the special case of $b = 0$, while angularity cross sections for any other value of b get factorized and resummed in $\mathrm{SCET_I}$. Such a comprehensive picture has been lacking so far for recoil-sensitive angularities measured with respect to the thrust axis. In this paper we make the first step to fill this gap and propose $\mathrm{SCET_{II}}$ factorization as a universal setup to calculate angularity distributions over the whole range of exponents b. Our forthcoming analysis of resummation [32] will provide important complementary information to validate this approach.

The plan of the paper is as follows. In section 2 we present a *broadening-like* factorization theorem for generic angularities with respect to the thrust axis, define the relevant jet and soft functions and compare our theoretical framework based on $\mathrm{SCET_{II}}$ against *thrust-like* factorization. In sections 3 and 4 we calculate bare angularity jet and soft functions to one-loop order in α_s, for arbitrary values of b, discuss the origin and nature of divergences and how these cancel in the cross section. In sections 3.3 and 4.3, it is shown how these functions reduce to the known broadening jet and soft functions in the limits $b \to 0^{\pm}$. Section 5 is devoted to the calculation of the one-loop hemisphere double-differential and single-differential angularity cross sections and to an analysis of the small-τ small-b limit, which requires special care and is shown to smoothly connect with the jet broadening limit. In section 5, we also derive the thrust limit ($b \to 1$) of our expressions and provide a comparison with the thrust-like factorization results from ref. [15] for $b \geq 1$. There we will show the additional contributions (sub-leading singular terms and power corrections) that our $\mathrm{SCET_{II}}$ approach allows us to work out. The most technical details of our calculations are left to the appendices. The comparison of our results against Event2 is the subject of section 6. We present our conclusions in section 7.

2 Factorization theorems for angularities with respect to the thrust axis

The focus of our analysis is on the effects of recoil of soft against collinear radiation in angularity distributions with respect to the thrust axis, for the whole range of angularity exponents. Jet broadening is the prototype of a recoil-sensitive angularity and its factorization theorem accounts for these effects. Starting from the generalization of the jet broadening factorization theorem to the case of angularity exponents away from $b = 0$, we will calculate recoil effects and show how (and by how much) they get suppressed if one approaches the thrust limit ($b = 1$) or takes $b > 1$. Furthermore, using this approach we will explore also the regime of negative values of b.

The factorization theorem for jet broadening was thoroughly discussed in refs. [34, 42]. In the following, we will use the notation of ref. [34], where the factorization formula was obtained using the $\mathrm{SCET_{II}}$ formalism. For angularities away from $b = 0$, one can repeat the same derivation with two modifications. First, the definition of the observable obviously changes. Secondly, the scaling of the gluon fields in the soft Wilson line becomes

JHEP08(2019)144

$A_s \sim Q(\lambda^{1+b}, \lambda^{1+b}, \lambda^{1+b})$. When b is close to zero, soft gluons throw collinear quarks off-shell and get encoded into a soft Wilson line $S_{n,\bar{n}}$ [30], as in the case of jet broadening. When $b \geq 1$, the gluons approach ultrasoft scaling and decouple from collinear quarks via a field redefinition yielding an ultrasoft Wilson line $Y_{n,\bar{n}}$ [30], as in the case of thrust factorization. In either case, (ultra)soft gluons decouple from collinear quarks/antiquarks to give (ultra)soft Wilson line factors, thereby leading to a factorization theorem of the same form, up to transverse-momentum dependence accounting for recoil of soft against collinear modes. In this paper, we will denote by $S_{n,\bar{n}}$ both of these Wilson lines in the fundamental representation entering the definition of the soft function.

Following and adapting the derivation in ref. [34], the *broadening-like* factorization theorem for the double-differential hemisphere angularity distribution with generic exponent b, is given by

$$\begin{aligned}\frac{1}{\sigma_0}\frac{\mathrm{d}\sigma}{\mathrm{d}\tau_L \mathrm{d}\tau_R} =& H(Q;\mu)\int \mathrm{d}\tau_n\, \mathrm{d}\tau_{\bar{n}}\, \mathrm{d}\tau_n^s\, \mathrm{d}\tau_{\bar{n}}^s\, \delta(\tau_R - \tau_n - \tau_n^s)\, \delta(\tau_L - \tau_{\bar{n}} - \tau_{\bar{n}}^s) \int \mathrm{d}\vec{p}_\perp^{\,2}\, \mathrm{d}\vec{k}_\perp^{\,2} \\ & \mathcal{J}(\tau_n, \vec{p}_\perp^{\,2}; \mu, \nu/Q)\, \mathcal{J}(\tau_{\bar{n}}, \vec{k}_\perp^{\,2}; \mu, \nu/Q)\, \mathcal{S}(\tau_n^s, \tau_{\bar{n}}^s, \vec{p}_\perp^{\,2}, \vec{k}_\perp^{\,2}; \mu, \nu)\,,\end{aligned} \tag{2.1}$$

where the contributions to the hemisphere angularities from soft and collinear sectors are denoted by τ_n^s, $\tau_{\bar{n}}^s$, τ_n and $\tau_{\bar{n}}$, respectively. The definitions of the jet and the soft functions are more general than for the jet broadening case in ref. [34] since the scaling of kinematical quantities, the fields and the measurement operator are all b-dependent. For notational convenience, this dependence is not written explicitly. The bare angularity jet function for a jet in the $\hat{n}$-hemisphere, in d space-time dimensions (with $d = 4 - 2\epsilon$) is

$$\mathcal{J}(\tau_n, \vec{p}_\perp^{\,2}) = \frac{(2\pi)^{3-2\epsilon}}{N_c}\mathrm{tr}\langle 0|\frac{\bar{\not{n}}}{2}\chi_n(0)\delta(Q - \bar{n}\cdot\hat{\mathcal{P}})\,\delta(\tau_n - \hat{\tau}_{\hat{n}})\delta^{(2-2\epsilon)}(\vec{p}_\perp - \hat{\mathcal{P}}_\perp)\bar{\chi}_n(0)|0\rangle\,, \tag{2.2}$$

where the operator $\hat{\tau}_{\hat{n}}$ measures the angularity on the final-state n-collinear jet. $\hat{\mathcal{P}}$ denotes the label momentum operator [29, 30] and χ_n is the collinear quark field [29, 30].[7] The jet function for the $\hat{\bar{n}}$-hemisphere is simply obtained through the replacement $n \to \bar{n}$ in eq. (2.2).

The bare angularity soft function, $\mathcal{S}(\tau_n^s, \tau_{\bar{n}}^s, \vec{p}_\perp^{\,2}, \vec{k}_\perp^{\,2})$ in eq. (2.1) is given by the following matrix element of Wilson lines $S_{n,\bar{n}}$,

$$\begin{aligned}\mathcal{S}(\tau_n^s, \tau_{\bar{n}}^s, \vec{p}_\perp^{\,2}, \vec{k}_\perp^{\,2}) =& \frac{\pi^{2-2\epsilon}(\vec{p}_\perp^{\,2})^{-\epsilon}(\vec{k}_\perp^{\,2})^{-\epsilon}}{N_c\,\Gamma^2(1-\epsilon)}\,\mathrm{tr}\langle 0|S_{\bar{n}}^\dagger(0)\,S_n(0)\,\delta^{(2-2\epsilon)}(\vec{p}_\perp + \mathbb{P}_{n\perp})\,\delta(\tau_n^s - \hat{\tau}_{\hat{n}}^s) \\ & \delta^{(2-2\epsilon)}(\vec{k}_\perp + \bar{\mathbb{P}}_{n\perp})\,\delta(\tau_{\bar{n}}^s - \hat{\tau}_{\hat{\bar{n}}}^s)\,S_n^\dagger(0)\,S_{\bar{n}}(0)|0\rangle\,,\end{aligned} \tag{2.3}$$

which is also a generalization of the broadening soft function in [34] in the sense that the soft Wilson line is now obeying the scaling suitable for a generic angularity, with $A_s \sim Q(\lambda^{1+b}, \lambda^{1+b}, \lambda^{1+b})$ rather than $A_s \sim Q(\lambda, \lambda, \lambda)$ specific to broadening. Here, $\mathbb{P}_{n\perp}$ and $\bar{\mathbb{P}}_{n\perp}$ are the operators that measure the net transverse momentum of all the particles

[7] Since the angularity distribution is gauge invariant, we can always choose a non-singular gauge to carry out our calculations, thereby avoiding the inclusion of T-Wilson lines [43] in the definition of SCET matrix elements.

JHEP08(2019)144

within a hemisphere [34]. The crucial point is that, whether the gluon field scaling in a Wilson line is more soft- or ultrasoft-like, the transverse momentum convolutions between jet and soft sectors will be kept. This allows us to include the effects of recoil at any intermediate stage of the calculation.

The hard function $H(Q;\mu)$ in eq. (2.1) instead, is identical to the cases of thrust and broadening. It encodes virtual corrections in the $q\bar{q}$ production at the hard scale Q, and is given by the squared Wilson coefficient of the matching of QCD onto SCET currents [44, 45]. Up to order α_s,

$$H(Q;\mu) = 1 + \frac{\alpha_s(\mu) C_F}{\pi}\left(-\frac{1}{\epsilon^2} - \frac{1}{\epsilon}\ln\frac{\mu^2}{Q^2} - \frac{3}{2\,\epsilon} - 4 + \frac{7\,\pi^2}{12} - \frac{1}{2}\ln^2\frac{\mu^2}{Q^2} - \frac{3}{2}\ln\frac{\mu^2}{Q^2}\right), \quad (2.4)$$

where we have explicitly included the ultraviolet (UV) divergences of the bare hard function calculated using dimensional regularization.

Hard, jet and soft functions depend upon the UV renormalization scale μ according to the familiar μ-renormalization group equations (RGEs). In addition to μ, the jet and the soft functions also depend upon the renormalization scale ν tied to rapidity divergences. In eq. (2.1), both μ- and ν-scale dependences cancel out among the individual functions order by order in perturbation theory, up to a residual μ-dependence at higher orders in α_s. The study of the renormalization group evolution of $\mathrm{SCET_{II}}$ angularity jet and soft functions is beyond the scope of this paper and will be the subject of a future publication [32].

We now discuss how the *thrust-like* factorization theorem in [15] follows from eq. (2.1). From the definition of the jet function we note that the transverse momenta $\vec{p}_\perp$ and $\vec{k}_\perp$ involved in the convolutions have the scaling of label momenta, and are thus expected to be of order λ. In the case of thrust ($b = 1$), the operators $\mathbb{P}_{n\perp}$ and $\bar{\mathbb{P}}_{n\perp}$ in the soft function of eq. (2.3), measure the transverse momentum of ultrasoft modes, which scales like λ^2. This is the scaling of residual momenta, which is suppressed compared to $\vec{p}_\perp$ and $\vec{k}_\perp$. Dropping correspondingly the operators $\mathbb{P}_{n\perp}$ and $\bar{\mathbb{P}}_{n\perp}$ in the δ-functions of eq. (2.3), one can factor $\delta^{(2-2\epsilon)}(\vec{p}_\perp)\delta^{(2-2\epsilon)}(\vec{k}_\perp)$ out of the soft function and perform the $\vec{p}_\perp^{\,2}$ and $\vec{k}_\perp^{\,2}$ integrals in the factorization theorem. This reduces the jet and the soft functions of eqs. (2.2) and (2.3), respectively, to

$$\begin{aligned}
\mathcal{J}(\tau_n) &= \frac{(2\pi)^{3-2\epsilon}}{N_c}\mathrm{tr}\langle 0|\frac{\bar{\not{n}}}{2}\chi_n(0)\delta(Q-\bar{n}\cdot\hat{\mathcal{P}})\,\delta(\tau_n-\hat{\tau}_{\bar{n}})\delta^{(2-2\epsilon)}(\hat{\mathcal{P}}_\perp)\bar{\chi}_n(0)|0\rangle\,,\\
\mathcal{S}(\tau_n^s,\tau_{\bar{n}}^s) &= \frac{1}{N_c}\,\mathrm{tr}\langle 0|S_{\bar{n}}^\dagger(0)\,S_n(0)\,\delta(\tau_n^s-\hat{\tau}_n^s)\delta(\tau_{\bar{n}}^s-\hat{\tau}_{\bar{n}}^s)\,S_n^\dagger(0)\,S_{\bar{n}}(0)|0\rangle\,,
\end{aligned} \quad (2.5)$$

which are the well-known jet and soft functions for thrust. The presence of $\delta^{(2-2\epsilon)}(\hat{\mathcal{P}}_\perp)$ in the thrust jet function ensures that the total transverse momentum of the particles in each hemisphere is zero. The factorization formula for the double-differential hemisphere thrust distribution in the dijet limit is well-known,

$$\begin{aligned}
\frac{1}{\sigma_0}\frac{\mathrm{d}\sigma}{\mathrm{d}\tau_L\mathrm{d}\tau_R} = H(Q;\mu)\int &\mathrm{d}\tau_n\,\mathrm{d}\tau_{\bar{n}}\,\mathrm{d}\tau_n^s\,\mathrm{d}\tau_{\bar{n}}^s\;\delta(\tau_R-\tau_n-\tau_n^s)\,\delta(\tau_L-\tau_{\bar{n}}-\tau_{\bar{n}}^s)\\
&\times\;\mathcal{J}(\tau_n;\mu)\,\mathcal{J}(\tau_{\bar{n}};\mu)\,\mathcal{S}(\tau_n^s,\tau_{\bar{n}}^s;\mu)\,,
\end{aligned} \quad (2.6)$$

JHEP08(2019)144

see e.g. [2, 46] for a derivation using the $\mathrm{SCET_I}$ formalism. If recoil effects are negligible, one can repeat the argument (adapting momentum scalings, measurement functions as well as the definitions of jet and soft functions) to derive a thrust-like factorization formula for double-differential angularity cross sections [13], which looks exactly like eq. (2.6) (see ref. [15]) in the same way eq. (2.1) looks like the factorization formula for jet broadening.

In section 5 we will show that when $b > 0$, the angularity distributions derived from the general, broadening-like factorization theorem contain all the singular terms from thrust-like factorization obtained in [15] together with suppressed singular terms and power corrections. In particular, we will show that at one-loop, the single-differential angularity cross section for strictly positive (and not vanishingly small) values of b, obtained from eq. (2.1), has the form

$$\left[\frac{1}{\sigma_0}\frac{\mathrm{d}\sigma^{(+)}}{\mathrm{d}\tau}\right]^{\mathcal{O}(\alpha_s)}_{\mathrm{SCET_{II}}} = \frac{\alpha_s(\mu)\,C_F}{\pi}\left\{A^{(+)}(b)\,\delta(\tau) - \frac{3}{1+b}\left[\frac{1}{\tau}\right]_+ - \frac{4}{1+b}\left[\frac{\ln\tau}{\tau}\right]_+ - \frac{4}{1+b}\frac{\ln(1-r)}{\tau}\right\}, \tag{2.7}$$

where σ_0 is the Born cross section, whose expression can be found e.g. in appendix A of ref. [4], $A^{(+)}(b)$ is b-dependent constant given in eq. (5.14) and r is the solution of the equation

$$\frac{r}{(1-r)^{1+b}} = \tau^b\,. \tag{2.8}$$

The first three terms in eq. (2.7) agree with the one-loop singular result from thrust-like factorization [15], while the last term gives the recoil effects due to $\mathrm{SCET_{II}}$ factorization theorem. Formally, this term, which we will refer to as *recoil correction* henceforth, is an integrable singularity for $0 < b < 1$, but of significant numerical size, as will be shown in section 6. Interestingly, the recoil correction reduces to a power correction in the thrust limit ($b \to 1$) and becomes singular in the broadening limit ($b \to 0$), thus smoothly connecting the singular thrust and broadening cross-section formulas at one loop. This will be shown in section 5. In the small-τ limit, the recoil correction can be expanded in powers of τ^b as

$$\frac{\ln(1-r)}{\tau} = \sum_{n=1}^{\lceil 1/b\rceil - 1}\frac{c_n}{\tau^{1-n\,b}} + \text{power corrections}\,. \tag{2.9}$$

Here the symbol $\lceil x\rceil$ denotes the *ceiling function*, making $(\lceil 1/b\rceil - 1)$ the greatest integer strictly smaller than $1/b$. The summation, with coefficients c_n dependent only on b, provides singular contributions for $0 < b < 1$. The singularity $1/\tau^{1-nb}$ is less severe than $1/\tau$ but more severe than $\ln\tau$, and thus we refer to it as a sub-leading singularity. Since this is integrable, it does not require a plus prescription. The appearance of fractional powers in the one-loop cross section is unique to angularities and is due to the recoil effects. While it is customary in the effective field theory approach to drop power corrections and keep only terms that are homogenous in power counting, here we cannot drop the recoil effect as a power correction, since it is produced by the leading-power $\mathrm{SCET_{II}}$ Lagrangian and is an artefact of the inhomogenous scaling of recoiling transverse momenta of the jet and soft functions. Indeed, the net transverse momentum of the jet function is equal and opposite

JHEP08(2019)144

to the net transverse momentum of the soft function, making its scaling ambiguous for an arbitrary b: one can choose it to scale like λ or λ^{1+b}. When $b \sim 1$, a multipole expansion in powers of $p_\perp^2$ reduces the factorization theorem to that of thrust-like angularities and consistently reduces the recoil correction to power correction which is numerically small. For small b the ambiguity is inherent in the problem and leads to inhomogeneity in the power counting. The recoil correction is numerically significant compared to the singular terms, it reduces to a singular term in small-b limit and modulates smoothly between the thrust and broadening limits. Thus one should consider this term as a leading correction due to recoil.

We stress that for $0.5 < b < 1$, our one-loop angularity distribution contains one new (sub-leading) singular contribution compared to the thrust-like computation that scales like τ^{1-b}. Since this contribution diverges for $\tau \to 0$ and is numerically sizable, this term will require a resummation to all orders in perturbation theory, which will be discussed in [32].

Similarly, for the case of strictly negative (and not vanishingly small) values of b, we will show that the one-loop single-differential angularity cross section has the form

$$\left[\frac{1}{\sigma_0}\frac{\mathrm{d}\sigma^{(-)}}{\mathrm{d}\tau}\right]^{\mathcal{O}(\alpha_s)}_{\mathrm{SCET_{II}}} = \frac{\alpha_s(\mu)\, C_F}{\pi}\left\{A^{(-)}(b)\,\delta(\tau) - \frac{3}{1+b}\left[\frac{1}{\tau}\right]_+ - \frac{4}{(1+b)^2}\left[\frac{\ln\tau}{\tau}\right]_+ - \frac{4}{(1+b)^2}\frac{\ln(1-s)}{\tau}\right\}, \tag{2.10}$$

where the b-dependent constant $A^{(-)}(b)$ is given in eq. (5.30) of section 5 and s is given by the solution of the equation

$$\frac{s}{(1-s)^{\frac{1}{1+b}}} = \tau^{-\frac{b}{1+b}}\,. \tag{2.11}$$

In the small-τ limit, the last term of eq. (2.10) can be expanded in powers of $\tau^{-\frac{b}{1+b}}$ as

$$\frac{\ln(1-s)}{\tau} = \sum_{n=1}^{\lceil 1/|b|\rceil - 2} \frac{c_n'}{\tau^{1+\frac{n\,b}{1+b}}} + \text{power corrections}\,, \tag{2.12}$$

where $(\lceil 1/|b|\rceil - 2)$ gives the greatest integer strictly smaller than $1/|b| - 1$. This result for angularity exponents $b < 0$ (or $a > 1$) is similar in structure to eq. (2.7), where the terms in the summation are sub-leading integrable singularities for $-1/2 < b < 0$. Although the sub-leading terms are power-suppressed in comparison to the leading singular terms, they cannot be expanded away as these terms are produced by the leading-order $\mathrm{SCET_{II}}$ Lagrangian and capture important recoil contributions. Moreover, the $\ln(1-s)/\tau$ term becomes a leading singularity in $b \to 0$ limit and reproduces the well-known result of the singular broadening cross-section at one loop. Along with eq. (2.7), this makes the singular angularity cross section continuous at $b = 0$. The numerical significance of the sub-leading singular terms relative to the singular contributions is studied in section 6, where we show that the sub-leading singular terms progressively become a leading contribution as b increases from $-1/2$ to 0. Note that for $-1 < b < -1/2$, all terms in the summation contribute as power corrections. In section 5 we will derive both eq. (2.7) and eq. (2.10) and will demonstrate the smoothness of the cross section at $b = 0$. The importance of the resummation of sub-leading singular terms will be addressed in a future publication [32].

JHEP08(2019)144

3 Angularity jet function at one loop

In this section, we present our results for the angularity jet function to one-loop order in α_s using the definition given in eq. (2.2), which includes the recoil effects. We cover both cases of positive-b and negative-b angularities for $b > -1$. This calculation is unique in many ways. Unlike the calculation of thrust and broadening jet functions the zero-bin contributions are non-vanishing here. There is an interesting interplay of zero-bin and rapidity divergences, due to which the jet function for positive b has an overall rapidity divergence while for negative b, the rapidity divergences cancel between the unsubtracted and zero-bin contributions to the jet function. We stress that these rapidity divergences are not regulated by the angularity exponent b. Moreover, the presence of rapidity divergences and rapidity logarithms in the one-loop jet function makes the calculation for an arbitrary angularity exponent b highly non-trivial.

3.1 Angularity jet function at one-loop for $b > 0$

Using the definition of the bare quark jet function given in eq. (2.2), the tree-level jet function corresponding to the quark jet in the right hemisphere (R) is given by

$$\mathcal{J}^{(0)}(\tau_R, \vec{p}_\perp^{\,2}) = \delta\left(\tau_R - \left(\frac{|\vec{p}_\perp|}{Q}\right)^{1+b}\right). \tag{3.1}$$

The other jet function corresponding to the left hemisphere (L) is obtained through the replacements $\tau_R \to \tau_L$ and $\vec{p}_\perp^{\,2} \to \vec{k}_\perp^{\,2}$.

We compute the one-loop jet function only for the case $\vec{p}_\perp = 0$ since this suffices for the computation of the cross section both at one-loop and up to NLL accuracy.[8] Indeed, the convolution of the one-loop jet function with the tree-level soft function, which is proportional to $\delta(\vec{p}_\perp^{\,2})\,\delta(\vec{k}_\perp^{\,2})$ (see eq. (4.1)), sets the net transverse momentum of the jet equal to zero. The results for the NLL resummed angularity distributions from broadening-like factorization will be presented in [32].

The relevant one-loop diagrams are those shown in figure 2, together with mirror images for graphs (b), (c) and (d). The diagrams in figure 2 are similar to the case of thrust, broadening or other similar di-jet observables, however the results computed below cannot be obtained from any of these known calculations because of non-trivial zero-bin and rapidity divergences due to the dependence on the exponent b.

We use the η-regulator as proposed in [34, 41] for regulating rapidity divergences and dimensional regularization for both UV and infrared (IR) divergences. Calculations in the following are performed in Feynman gauge. However, the results we obtained are valid for any choice of covariant gauge owing to collinear gauge invariance of the jet function [34]. Virtual correction diagrams (c) and (d) are given by scaleless integrals and hence vanish in pure dimensional regularization. Diagram (e) is zero in Feynman gauge. The bare one-loop jet function is thus given as the sum of the contributions from diagrams (a) and

[8] Beyond this order, one would require the one-loop jet function with full $\vec{p}_\perp$ dependence, which is beyond the scope of this work.

JHEP08(2019)144

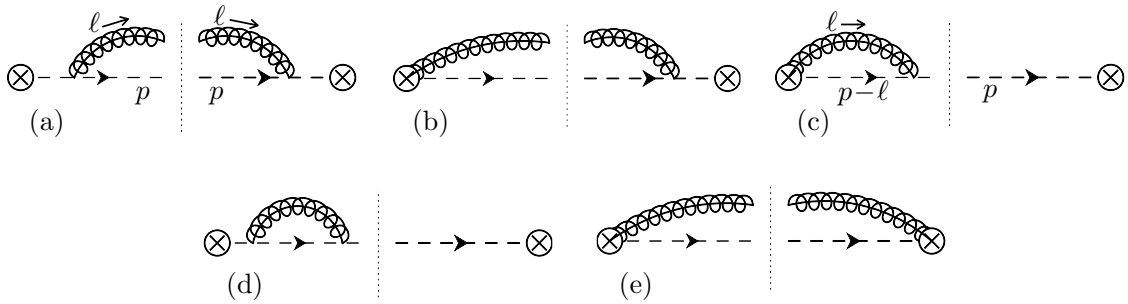

Figure 2. Diagrams contributing to the angularity jet function at one-loop order. Here, p^μ is the quark momentum and l^μ is the gluon momentum. The mirror image graphs for (b), (c) and (d) are not shown here. Diagram (d) denotes the quark wave-function renormalization contribution.

(b) together with corresponding zero-bin subtractions [47], which remove double counting between jet and soft regions.

Diagram (a) does not require any rapidity regulator. The zero-bin contribution for this graph is given by a scaleless integral and thus vanishes in pure dimensional regularization. We refer to appendix B.1 for details of our calculation. The bare jet diagram (a) is given by

$$\mathcal{J}_{\rm a}^{(1)}(\tau_R,0) = \frac{\alpha_s(\mu)C_F}{\pi}\frac{e^{\epsilon\gamma_E}}{\Gamma(1-\epsilon)}\Big(\frac{\mu}{Q}\Big)^{2\epsilon}\frac{1}{\tau_R^{1+\frac{2\epsilon}{1+b}}}\,\frac{1-\epsilon}{1+b}\int_0^1 \mathrm{d}x\, x\,[(1-x)^{-b}+x^{-b}]^{\frac{2\epsilon}{1+b}}\,, \tag{3.2}$$

where $x = l^-/Q$ is the light-cone momentum fraction of the radiated gluon. The factor $1/\tau^{1+\beta}$ should be interpreted as a plus distribution with infinity boundary, satisfying the condition $\int_0^\infty \mathrm{d}\tau\,\Big[1/\tau^{1+\beta}\Big]_+^\infty = 0$. The definition of this distribution and related useful identities are collected in appendix A.1. We expand the result in eq. (3.2) in powers of ϵ to identify divergent and finite parts,

$$\mathcal{J}_{\rm a}^{(1)}(\tau_R,0) = \frac{\alpha_s(\mu)C_F}{\pi}\Big[-\frac{1}{4\,\epsilon}\,\delta(\tau_R)+\frac{1}{2(1+b)}\frac{1}{m}\Big[\frac{1}{\tau_R/m}\Big]_+ + i_a\,\delta(\tau_R)+\mathcal{O}(\epsilon)\Big], \tag{3.3}$$

where

$$i_a = \frac{1}{4(1+b)} - \frac{1}{1+b}\int_0^1 \mathrm{d}x\, x\,\ln\Big(1+\Big(\frac{x}{1-x}\Big)^b\Big)\,, \tag{3.4}$$

and $m = (\mu/Q)^{1+b}$. Here $[1/\tau]_+$ denotes the plus distribution with boundary at $\tau = +1$, see appendix A.1.

For the jet diagram (b), we include a factor of 2 to account for its mirror image. Moreover, as we are going to show, diagram (b) also yields a non-vanishing zero-bin subtraction. The result of the unsubtracted jet diagram (b) is

$$\mathcal{J}_{\rm b,unsub}^{(1)}(\tau_R,0) = \frac{2}{1+b}\frac{\alpha_s(\mu)C_F}{\pi}\frac{e^{\epsilon\gamma_E}w^2}{\Gamma(1-\epsilon)}\Big(\frac{\mu}{Q}\Big)^{2\epsilon}\Big(\frac{\nu}{Q}\Big)^{\eta}\frac{1}{\tau_R^{1+\frac{2\epsilon}{1+b}}}\int_0^1 \mathrm{d}x[(1-x)^{-b}+x^{-b}]^{\frac{2\epsilon}{1+b}}\frac{(1-x)}{x^{1+\eta}}, \tag{3.5}$$

where ν is the rapidity renormalization scale and w is a bookkeeping parameter to keep track of the rapidity divergences.[9] Details of the calculation are presented in appendix B.2.1.

[9] $w = 1+\mathcal{O}(\eta)$ and will be important for obtaining the renormalization group equations.

JHEP08(2019)144

Here again, we expand the integrand in the regulators η and ϵ before evaluating the integral, as in the case of jet diagram (a). We stress that the full ϵ-dependence must be retained in the term containing the rapidity divergence as discussed in ref. [34] and the proper order in taking the limits must be $\eta \to 0$, then $\epsilon \to 0$ with $\eta/\epsilon^n \to 0$ for all $n > 0$. The unsubtracted result for the jet diagram (b) exhibits a singularity at $x \to 0$ which is regulated by η. However, a careful examination of the integral shows that η is required to regulate the divergence at $x \to 0$ only when $b \leq 0$. Hence, the η-regulator can be safely dropped for positive-b angularities, as the $x \to 0$ limit in this case is already regulated by ϵ. Thus for $b > 0$, we get

$$\begin{aligned}\mathcal{J}^{(1+)}_{b,\text{unsub}}(\tau_R,0) = \frac{\alpha_s(\mu)\,C_F}{\pi}\Bigg[&\frac{1+b}{2\,b\,\epsilon^2}\,\delta(\tau_R) + \frac{1}{\epsilon}\delta(\tau_R) - \frac{1}{b\,\epsilon}\frac{1}{m}\left[\frac{1}{\tau_R/m}\right]_+ + \frac{2}{b(1+b)}\frac{1}{m}\left[\frac{\ln(\tau_R/m)}{\tau_R/m}\right]_+ \\ &- \frac{2}{1+b}\frac{1}{m}\left[\frac{1}{\tau_R/m}\right]_+ - \frac{2}{1+b}\,\delta(\tau_R)\int_0^1 \mathrm{d}x\,\frac{(1-x)}{x}\ln\left(1+\left(\frac{x}{1-x}\right)^b\right) \\ &- \frac{\pi^2}{24}\frac{1+b}{b}\,\delta(\tau_R) + \frac{2\,b}{1+b}\,\delta(\tau_R) + \mathcal{O}(\epsilon)\Bigg],\end{aligned} \tag{3.6}$$

with, $m = (\mu/Q)^{1+b}$ as before. The zero-bin contribution $\mathcal{J}^{(1+)}_{\text{b},0}$ for this graph is obtained by taking the gluon momentum to scale as $l^\mu \sim Q(\lambda^{1+b}, \lambda^{1+b}, \lambda^{1+b})$. For the explicit calculation we refer to appendix B.3. We obtain

$$\mathcal{J}^{(1+)}_{\text{b},0}(\tau_R,0) = \frac{2}{1+b}\frac{\alpha_s(\mu)C_F}{\pi}\frac{e^{\epsilon\gamma_E}}{\Gamma(1-\epsilon)}w^2\left(\frac{\nu}{Q}\right)^\eta\left(\frac{\mu}{Q}\right)^{2\epsilon}\frac{1}{\tau_R^{1+\frac{2\epsilon}{1+b}}}\frac{\Gamma\left(\frac{\eta}{b}\right)\Gamma\left(-\frac{2\epsilon}{1+b}-\frac{\eta}{b}\right)}{b\,\Gamma\left(-\frac{2\epsilon}{1+b}\right)}, \tag{3.7}$$

which upon expansion in η and then in ϵ unveils the rapidity divergence,

$$\begin{aligned}\mathcal{J}^{(1+)}_{b,0}(\tau_R,0) = \frac{\alpha_s(\mu)\,C_F}{\pi}\Bigg[&\frac{2w^2\,e^{\epsilon\,\gamma_E}}{\eta\,(1+b)\,\Gamma(1-\epsilon)}\left(\frac{\mu}{Q}\right)^{2\epsilon}\left[\frac{1}{\tau_R^{1+\frac{2\epsilon}{1+b}}}\right]_+^\infty + \frac{1+b}{2\,b\,\epsilon^2}\,\delta(\tau_R) - \frac{1}{b\,\epsilon}\frac{1}{m}\left[\frac{1}{\tau_R/m}\right]_+ \\ &- \frac{1}{\epsilon}\ln\frac{\nu}{Q}\,\delta(\tau_R) + \frac{2}{b(1+b)}\frac{1}{m}\left[\frac{\ln(\tau_R/m)}{\tau_R/m}\right]_+ + \frac{2}{1+b}\ln\frac{\nu}{Q}\frac{1}{m}\left[\frac{1}{\tau_R/m}\right]_+ \\ &- \frac{\pi^2}{24\,b}\frac{b^2+2\,b+9}{1+b}\,\delta(\tau_R) + \mathcal{O}(\eta,\epsilon)\Bigg].\end{aligned} \tag{3.8}$$

The total contribution of diagram (b) including the zero-bin subtraction for $b > 0$ is then

$$\begin{aligned}\mathcal{J}^{(1+)}_b(\tau_R,0) &= \mathcal{J}^{(1+)}_{b,\text{unsub}}(\tau_R,0) - \mathcal{J}^{(1+)}_{\text{b},0}(\tau_R,0) \\ &= \frac{\alpha_s(\mu)C_F}{\pi}\Bigg[-\frac{2\,w^2\,e^{\epsilon\gamma_E}}{\eta\,(1+b)\,\Gamma(1-\epsilon)}\left(\frac{\mu}{Q}\right)^{2\epsilon}\left[\frac{1}{\tau_R^{1+\frac{2\epsilon}{1+b}}}\right]_+^\infty + \frac{1}{\epsilon}\ln\frac{\nu}{Q}\,\delta(\tau_R) + \frac{1}{\epsilon}\,\delta(\tau_R) \\ &\quad - \frac{2}{1+b}\ln\frac{\nu}{Q}\frac{1}{m}\left[\frac{1}{\tau_R/m}\right]_+ - \frac{2}{1+b}\frac{1}{m}\left[\frac{1}{\tau_R/m}\right]_+ - i_b^{(+)}\,\delta(\tau_R) + \mathcal{O}(\eta,\epsilon)\Bigg],\end{aligned} \tag{3.9}$$

JHEP08(2019)144

where

$$i_b^{(+)} = \frac{2}{1+b}\int_0^1 \mathrm{d}x\,\frac{(1-x)}{x}\ln\left(1+\left(\frac{x}{1-x}\right)^b\right) - \frac{2\,b}{1+b} - \frac{\pi^2}{3\,b(1+b)}\,. \tag{3.10}$$

It is interesting to note that the zero-bin plays an important role in this calculation. In the case of the broadening jet function in ref. [34], the rapidity divergence emerged from the unsubtracted equivalent of diagram (b) and the zero-bin vanished, using the same regulators and gauge as done here. Instead, for positive-b angularities the rapidity divergence emerges from the zero-bin subtraction, which is non-vanishing.

Adding the results for diagram (a) and (b), we get the bare one-loop right-hemisphere jet function for positive-b angularities,

$$\begin{aligned}\mathcal{J}^{(1+)}(\tau_R,0) = \frac{\alpha_s(\mu)C_F}{\pi}\Bigg[&-\frac{2\,w^2\,e^{\epsilon\gamma_E}}{\eta\,(1+b)\,\Gamma(1-\epsilon)}\left(\frac{\mu}{Q}\right)^{2\epsilon}\left[\frac{1}{\tau_R^{1+\frac{2\epsilon}{1+b}}}\right]_+^\infty + \frac{1}{\epsilon}\ln\frac{\nu}{Q}\,\delta(\tau_R) + \frac{3}{4\,\epsilon}\,\delta(\tau_R)\\ &-\frac{2}{1+b}\ln\frac{\nu}{Q}\,\frac{1}{m}\left[\frac{1}{\tau_R/m}\right]_+ - \frac{3}{2(1+b)}\frac{1}{m}\left[\frac{1}{\tau_R/m}\right]_+ + (i_a - i_b^{(+)})\,\delta(\tau_R) + \mathcal{O}(\eta,\epsilon)\Bigg].\end{aligned} \tag{3.11}$$

The bare one-loop left-hemisphere jet function has the same form but with τ_R replaced by τ_L. We stress that both the angularity jet function and the soft function, as we are going to show, contain factors of $1/b$ which make them singular as $b \to 0$. The situation here is similar to what happens in the formalism of ref. [24] for angularities measured with respect to a recoil-insensitive axis. Their jet and soft functions still yielded a well-defined resummed cross section for small b due to the decreasing range of integration in the RG evolution [24]. The same feature will emerge in our case [32].

3.2 Angularity jet function at one-loop for $b < 0$

The tree-level jet function remains the same as given in eq. (3.1) for negative-b angularities. At one loop, the result for the jet diagram (a) also remains unchanged and the integral in eq. (3.4) is non-singular for both positive and negative-b values. Hence, the same expressions as eqs. (3.3) and (3.4) hold for all $b > -1$ angularities. However, as noted earlier, the unsubtracted jet integral for diagram (b) given in eq. (3.5) exhibits a singularity as $x \to 0$ and the η-regulator is essential to deal with this limit when $b \leq 0$. The result for the unsubtracted jet diagram (b) upon expansion in η and ϵ, for $-1 < b < 0$ is given by

$$\begin{aligned}\mathcal{J}^{(1-)}_{\mathrm{b,unsub}}(\tau_R,0) = \frac{\alpha_s(\mu)\,C_F}{\pi}\Bigg[&-\frac{2\,w^2\,e^{\epsilon\gamma_E}}{\eta\,(1+b)\,\Gamma(1-\epsilon)}\left(\frac{\mu}{Q}\right)^{2\epsilon}\left[\frac{1}{\tau_R^{1+\frac{2\epsilon}{1+b}}}\right]_+^\infty + \frac{1}{\epsilon}\ln\frac{\nu}{Q}\,\delta(\tau_R) + \frac{1}{\epsilon}\,\delta(\tau_R)\\ &-\frac{2}{1+b}\ln\frac{\nu}{Q}\,\frac{1}{m}\left[\frac{1}{\tau_R/m}\right]_+ - \frac{2}{1+b}\frac{1}{m}\left[\frac{1}{\tau_R/m}\right]_+ + \frac{2\,b}{1+b}\,\delta(\tau_R) - \frac{\pi^2\,b}{3(1+b)}\,\delta(\tau_R)\\ &-\frac{2}{1+b}\,\delta(\tau_R)\int_0^1 \mathrm{d}x\,\frac{(1-x)}{x}\ln\left(1+\left(\frac{x}{1-x}\right)^{-b}\right) + \mathcal{O}(\eta,\epsilon)\Bigg]\,.\end{aligned} \tag{3.12}$$

JHEP08(2019)144

The intermediate steps of the calculation can be found in appendix B.2.2. The zero-bin diagram flips sign for negative-b (see appendix B.3) leading to

$$\begin{aligned}
\mathcal{J}^{(1-)}_{(\mathrm{b},0)}(\tau_R,0) &= -\frac{2}{1+b}\frac{\alpha_s(\mu)C_F}{\pi}\frac{e^{\epsilon\gamma_E}}{\Gamma(1-\epsilon)}w^2\left(\frac{\nu}{Q}\right)^{\eta}\left(\frac{\mu}{Q}\right)^{2\epsilon}\frac{1}{\tau_R^{1+\frac{2\epsilon}{1+b}}}\frac{\Gamma(\frac{\eta}{b})\,\Gamma\left(-\frac{2\epsilon}{1+b}-\frac{\eta}{b}\right)}{b\,\Gamma\left(-\frac{2\epsilon}{1+b}\right)} \\
&= \frac{\alpha_s(\mu)\,C_F}{\pi}\Bigg[-\frac{2\,w^2\,e^{\epsilon\,\gamma_E}}{\eta(1+b)\Gamma(1-\epsilon)}\left(\frac{\mu}{Q}\right)^{2\epsilon}\left[\frac{1}{\tau_R^{1+\frac{2\epsilon}{1+b}}}\right]_+^{\infty}-\frac{1+b}{2\,b\,\epsilon^2}\,\delta(\tau_R)+\frac{1}{b\,\epsilon}\frac{1}{m}\left[\frac{1}{\tau_R/m}\right]_+ \\
&\quad+\frac{1}{\epsilon}\ln\frac{\nu}{Q}\,\delta(\tau_R)-\frac{2}{b(1+b)}\,\frac{1}{m}\left[\frac{\ln(\tau_R/m)}{\tau_R/m}\right]_+-\frac{2}{1+b}\,\ln\frac{\nu}{Q}\,\frac{1}{m}\left[\frac{1}{\tau_R/m}\right]_+ \\
&\quad+\frac{\pi^2}{24\,b}\,\frac{b^2+2\,b+9}{1+b}\,\delta(\tau_R)+\mathcal{O}(\eta,\epsilon)\Bigg]\,. \qquad (3.13)
\end{aligned}$$

The total contribution of diagram (b) for angularities with $b<0$ is then

$$\begin{aligned}
\mathcal{J}^{(1-)}_{\mathrm{b}}(\tau_R,0) &= \frac{\alpha_s(\mu)C_F}{\pi}\Bigg[\frac{1+b}{2b\epsilon^2}\,\delta(\tau_R)-\frac{1}{b\epsilon}\frac{1}{m}\left[\frac{1}{\tau_R/m}\right]_++\frac{1}{\epsilon}\delta(\tau_R)+\frac{2}{b(1+b)}\frac{1}{m}\left[\frac{\ln(\tau_R/m)}{\tau_R/m}\right]_+ \\
&\quad-\frac{2}{1+b}\,\frac{1}{m}\left[\frac{1}{\tau_R/m}\right]_+-\frac{\pi^2}{24}\,\frac{1+b}{b}\delta(\tau_R)-i_b^{(-)}\,\delta(\tau_R)+\mathcal{O}(\epsilon)\Bigg]\,, \qquad (3.14)
\end{aligned}$$

where

$$i_b^{(-)}=\frac{2}{1+b}\int_0^1\mathrm{d}x\,\frac{(1-x)}{x}\ln\left(1+\left(\frac{x}{1-x}\right)^{-b}\right)-\frac{2\,b}{1+b}+\frac{\pi^2}{3(1+b)}\left(\frac{b^2+1}{b}\right). \qquad (3.15)$$

Adding the contributions of diagrams (a) and (b), we obtain the bare jet function for $b<0$,

$$\begin{aligned}
\mathcal{J}^{(1-)}(\tau_R,0) &= \frac{\alpha_s(\mu)C_F}{\pi}\Bigg[\frac{1+b}{2b\epsilon^2}\delta(\tau_R)-\frac{1}{b\epsilon}\frac{1}{m}\left[\frac{1}{\tau_R/m}\right]_++\frac{3}{4\epsilon}\,\delta(\tau_R)+\frac{2}{b(1+b)}\frac{1}{m}\left[\frac{\ln(\tau_R/m)}{\tau_R/m}\right]_+ \\
&\quad-\frac{3}{2(1+b)}\frac{1}{m}\left[\frac{1}{\tau_R/m}\right]_+-\frac{\pi^2}{24}\frac{1+b}{b}\,\delta(\tau_R)+(i_a-i_b^{(-)})\,\delta(\tau_R)+\mathcal{O}(\eta,\epsilon)\Bigg]. \qquad (3.16)
\end{aligned}$$

It is interesting to note that the zero-bin graph exhibits a rapidity divergence for both positive-b and negative-b integrals. It is only the unsubtracted jet function graph (b) that does not contain any rapidity divergence for positive-b angularities. The negative-b angularity jet function has no net rapidity divergence as both the unsubtracted jet diagram and its zero-bin contain rapidity divergences which cancel in the sum. In addition, it contains ϵ-divergences proportional to $1/b$ which cancel against the soft function divergence (see eq. (4.13) below), as expected since the hard function is universal for any angularity.

3.3 Jet broadening limit of the one-loop jet function

We will now show that we are able to reproduce the jet broadening ($b=0$) jet function from our previous results. This provides a cross-check on our calculation. However, it is important to stress that one cannot retrieve the jet broadening limit from the angularity jet function *after* expanding in η and ϵ, as the limits $\eta,\epsilon\to 0$ do not commute with $b\to 0$.

JHEP08(2019)144

The unexpanded result of eq. (3.2) for the jet graph (a) in the limit $b \to 0^{\pm}$ reduces to

$$\lim_{b\to 0^{\pm}} \mathcal{J}_{\rm a}^{(1)}(\tau_R, 0) = \frac{\alpha_s(\mu) C_F}{\pi} \frac{e^{\epsilon\gamma_E}}{\Gamma(1-\epsilon)} \left(\frac{\mu}{Q}\right)^{2\epsilon} \left[\frac{1}{\tau_R^{1+2\epsilon}}\right]_+^{\infty} (1-\epsilon) \int_0^1 \mathrm{d}x\, x\, 2^{2\epsilon}$$
$$= \frac{\alpha_s(\mu) C_F}{2\pi} \frac{e^{\epsilon\gamma_E}}{\Gamma(1-\epsilon)} \left(\frac{2\,\mu}{Q}\right)^{2\epsilon} \left[\frac{1}{\tau_R^{1+2\epsilon}}\right]_+^{\infty} (1-\epsilon)\,. \tag{3.17}$$

The jet diagram (b) of eq. (3.5) including the zero-bin subtraction (see eq. (B.9)), in the limit $b \to 0^{\pm}$, gives

$$\lim_{b\to 0^{\pm}} \mathcal{J}_{\rm b}^{(1)}(\tau_R, 0)$$
$$= 2\, \frac{\alpha_s(\mu) C_F}{\pi} \frac{e^{\epsilon\gamma_E}\, w^2}{\Gamma(1-\epsilon)} \left(\frac{\mu}{Q}\right)^{2\epsilon} \left(\frac{\nu}{Q}\right)^{\eta} \left[\frac{1}{\tau_R^{1+2\epsilon}}\right]_+^{\infty} \left[\int_0^1 \mathrm{d}x\, 2^{2\epsilon} \frac{(1-x)}{x^{1+\eta}} - \int_0^{\infty} \mathrm{d}x \frac{1}{x^{1+\eta}}\, 2^{2\epsilon}\right]$$
$$= 2\, \frac{\alpha_s(\mu) C_F}{\pi} \frac{e^{\epsilon\gamma_E}\, w^2}{\Gamma(1-\epsilon)} \left(\frac{2\,\mu}{Q}\right)^{2\epsilon} \left(\frac{\nu}{Q}\right)^{\eta} \left[\frac{1}{\tau_R^{1+2\epsilon}}\right]_+^{\infty} \left[-\frac{1}{\eta} - 1 + \mathcal{O}(\eta)\right]. \tag{3.18}$$

Adding the contributions in eqs. (3.17) and (3.18), we get the one-loop jet function in the limit $b \to 0$,

$$\lim_{b\to 0} \mathcal{J}^{(1)}(\tau_R, 0) = \frac{\alpha_s(\mu) C_F}{2\pi} \frac{e^{\epsilon\gamma_E}}{\Gamma(1-\epsilon)} \left(\frac{2\,\mu}{Q}\right)^{2\epsilon} \left[\frac{1}{\tau_R^{1+2\epsilon}}\right]_+^{\infty} \left[(1-\epsilon) + 4\, w^2 \left(\frac{\nu}{Q}\right)^{\eta} \left(-\frac{1}{\eta} - 1\right)\right], \tag{3.19}$$

which agrees with the broadening jet function given in eq. (6.38) of ref. [34].

4 Angularity soft function at one loop

In this section, we present our calculation of the bare angularity soft function to one loop, based on the definition given in eq. (2.3). The one-loop soft function for angularities is a generalization of the one-loop soft function for the jet broadening case. However, the presence of the exponent b, not only makes the calculation significantly more difficult than in the case of jet broadening, but also the choice of distribution variables becomes highly non-trivial, due to the presence of coupled distributions. As in the case of the jet function and consistent with it, we find a net rapidity divergence for the soft function when $b > 0$, while no net rapidity divergence is present when $b < 0$. We provide novel one-loop results of the soft function for both the positive and the negative value of the angularity exponent.

4.1 Soft function calculation for $b > 0$

According to eq. (2.3), the tree-level soft function is simply given by

$$\mathcal{S}^{(0)}(\tau_L, \tau_R, \vec{p}_\perp^{\,2}, \vec{k}_\perp^{\,2}) = \delta(\tau_L)\, \delta(\tau_R)\, \delta(\vec{p}_\perp^{\,2})\, \delta(\vec{k}_\perp^{\,2})\,. \tag{4.1}$$

The relevant Feynman diagrams for the one-loop computation are shown in figure 3. As in the case of the jet function, we will use the η-regulator for rapidity divergences and dimensional regularization for both UV and IR divergences. Due to our choice of gauge, a non-zero contribution arises only when a gluon is exchanged between n-collinear and

JHEP08(2019)144

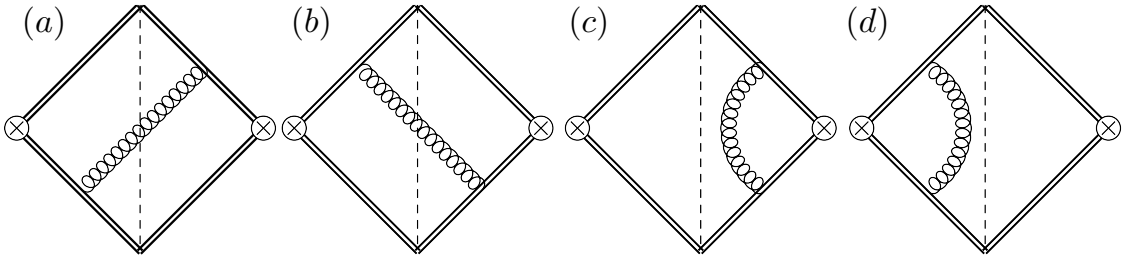

Figure 3. Diagrams contributing to the angularity soft function at one-loop order. Diagrams (a) and (b) give identical contribution due to symmetry.

$\bar{n}$-collinear Wilson lines. Virtual correction diagrams (c) and (d) are given by scaleless integrals and therefore vanish due to our choice of regulators. Since (a) and (b) give identical contributions, we only need to compute one diagram at this order. The details of this calculation are presented in appendix C. The bare one-loop soft function for all $b > -1$ is given by

$$\mathcal{S}^{(1)}(\tau_L, \tau_R, \vec{p}_\perp^2, \vec{k}_\perp^2) = \frac{\alpha_s(\mu)\, C_F}{\pi} \frac{\mu^{2\epsilon} e^{\epsilon\gamma_E}}{\Gamma(1-\epsilon)} \nu^\eta\, w^2\, Q\, \delta(\tau_L)\, \delta(\vec{k}_\perp^2)\, \theta\!\left(\left(\frac{|\vec{p}_\perp|}{Q\,\tau_R}\right)^{1/b} - 1\right)$$
$$\times\, (\vec{p}_\perp^2)^{\,-1-\epsilon-\frac{\eta+1}{2}} \frac{\left|1 - \left(\frac{Q\,\tau_R}{|\vec{p}_\perp|}\right)^{2/b}\right|^{-\eta}}{|b| \left(\frac{Q\,\tau_R}{|\vec{p}_\perp|}\right)^{1-\eta/b}} + \left\{ \begin{array}{c} \tau_L \leftrightarrow \tau_R \\ \vec{k}_\perp^2 \leftrightarrow \vec{p}_\perp^2 \end{array} \right\}. \tag{4.2}$$

The term $\theta\!\left(\left(\frac{|\vec{p}_\perp|}{Q\,\tau_R}\right)^{1/b} - 1\right) \left|1 - \left(\frac{Q\,\tau_R}{|\vec{p}_\perp|}\right)^{2/b}\right|^{-\eta}$ in this equation couples the variables $\tau_R(\tau_L)$ and $\vec{p}_\perp(\vec{k}_\perp)$. In order to avoid dealing with coupled distributions in τ_R and $\vec{p}_\perp$ (τ_L and $\vec{k}_\perp$), which are difficult to interpret, we perform a change of variables. Noting that the coupled Heaviside step function is equivalent to $\theta(|\vec{p}_\perp| - Q\,\tau_R)$ for $b > 0$, we introduce the variables

$$v_L = \frac{Q\tau_L}{k_\perp}\,, \qquad v_R = \frac{Q\tau_R}{p_\perp}\,, \tag{4.3}$$

where $p_\perp \equiv |\vec{p}_\perp|$ and $k_\perp \equiv |\vec{k}_\perp|$. Accordingly, for positive-b angularities,

$$\mathcal{S}^{(1+)}(\tau_L, \tau_R, \vec{p}_\perp^2, \vec{k}_\perp^2) = \mathcal{S}^{(1+)}(v_L, v_R, \vec{p}_\perp^2, \vec{k}_\perp^2) \left[\left|\frac{\mathrm{d}v_L}{\mathrm{d}\tau_L}\right| \left|\frac{\mathrm{d}v_R}{\mathrm{d}\tau_R}\right|\right]$$
$$= \frac{\alpha_s(\mu)\, C_F}{\pi} \frac{e^{\epsilon\gamma_E}}{\Gamma(1-\epsilon)}\, w^2 \left(\frac{\nu}{\mu}\right)^\eta \delta(v_L)\, \delta(\vec{k}_\perp^2)\, \frac{\theta(1-v_R)\,(1-v_R^{2/b})^{-\eta}}{b\, v_R^{1-\eta/b}}$$
$$\times\, \frac{1}{\mu^2} \frac{1}{(\vec{p}_\perp^2/\mu^2)^{1+\epsilon+\frac{\eta}{2}}} \left[\left|\frac{\mathrm{d}v_L}{\mathrm{d}\tau_L}\right| \left|\frac{\mathrm{d}v_R}{\mathrm{d}\tau_R}\right|\right] + \left\{ \begin{array}{c} v_L \leftrightarrow v_R \\ \vec{k}_\perp^2 \leftrightarrow \vec{p}_\perp^2 \end{array} \right\}, \tag{4.4}$$

where

$$\left|\frac{\mathrm{d}v_L}{\mathrm{d}\tau_L}\right| = \frac{Q}{k_\perp}\,, \qquad \left|\frac{\mathrm{d}v_R}{\mathrm{d}\tau_R}\right| = \frac{Q}{p_\perp}\,, \tag{4.5}$$

JHEP08(2019)144

which enter the Jacobian factor. Keeping track of Jacobian factors is necessary since the soft function is a distribution and its arguments represent the variables of the integration measure. Thanks to eq. (4.3), the expansions in η and ϵ give rise to decoupled distributions in v_R and $\vec{p}_\perp$ (v_L and $\vec{k}_\perp$). The distribution in v_R, upon expansion in η leads to

$$\left[\frac{\theta(1-v_R)(1-v_R^{2/b})^{-\eta}}{v_R^{1-\eta/b}}\right]_+^\infty = \theta(1-v_R)\left(\left[\frac{1}{v_R}\right]_+ + \frac{\eta}{b}\left[\frac{\ln v_R}{v_R}\right]_+ - \eta\left[\frac{\ln(1-v_R^{2/b})}{v_R}\right]_+\right) + a\,\delta(v_R) + \mathcal{O}(\eta^2), \tag{4.6}$$

where we follow the standard convention for plus distributions, i.e. $\int_0^1 \mathrm{d}x \left[\frac{\ln^n x}{x^{1+\alpha}}\right]_+ = 0 = \int_0^1 \mathrm{d}x \left[\frac{\ln^n(1-x^\alpha)}{x}\right]_+$. To fix the coefficient a of the $\delta(v_R)$ term, we integrate the above equation over v_R from 0 to 1, which leads to

$$\left[\frac{\theta(1-v_R)(1-v_R^{2/b})^{-\eta}}{v_R^{1-\eta/b}}\right]_+^\infty = \frac{b}{\eta}\,\delta(v_R) + \left[\frac{\theta(1-v_R)}{v_R}\right]_+ + \eta\left(\frac{\pi^2}{12}\,b\,\delta(v_R) + \frac{1}{b}\left[\frac{\theta(1-v_R)\ln v_R}{v_R}\right]_+ - \left[\frac{\theta(1-v_R)\ln(1-v_R^{2/b})}{v_R}\right]_+\right) + \mathcal{O}(\eta^2)\,. \tag{4.7}$$

The expansion in the regulators for the one-loop bare soft function thus gives

$$\begin{aligned}\mathcal{S}^{(1+)}(v_L, v_R, \vec{p}_\perp^2, \vec{k}_\perp^2) = \frac{\alpha_s(\mu)\,C_F}{\pi}\Bigg\{&\frac{w^2\,e^{\epsilon\gamma_E}}{\eta\Gamma(1-e)}\frac{1}{\mu^2}\left[\frac{1}{(\vec{p}_\perp^2/\mu^2)^{1+\epsilon}}\right]_+^\infty \delta(v_R) - \frac{1}{b\,\epsilon}\left[\frac{\theta(1-v_R)}{v_R}\right]_+ \delta(\vec{p}_\perp^2)\\ &+ \delta(v_R)\,\delta(\vec{p}_\perp^2)\left(\frac{1}{2\epsilon^2} - \frac{1}{\epsilon}\ln\frac{\nu}{\mu}\right) - \frac{1}{2}\delta(v_R)\frac{1}{\mu^2}\left[\frac{\ln(\vec{p}_\perp^2/\mu^2)}{\vec{p}_\perp^2/\mu^2}\right]_+^{\mathcal{D}_\mu} + \ln\frac{\nu}{\mu}\,\delta(v_R)\,\frac{1}{\mu^2}\left[\frac{1}{\vec{p}_\perp^2/\mu^2}\right]_+^{\mathcal{D}_\mu}\\ &+ \frac{1}{b}\left[\frac{\theta(1-v_R)}{v_R}\right]_+ \frac{1}{\mu^2}\left[\frac{1}{\vec{p}_\perp^2/\mu^2}\right]_+^{\mathcal{D}_\mu} - \frac{\pi^2}{24}\delta(v_R)\,\delta(\vec{p}_\perp^2) + \mathcal{O}(\eta,\epsilon)\Bigg\}\,\delta(v_L)\,\delta(\vec{k}_\perp^2) + \left\{\begin{matrix} v_L \leftrightarrow v_R \\ \vec{k}_\perp^2 \leftrightarrow \vec{p}_\perp^2\end{matrix}\right\}.\end{aligned} \tag{4.8}$$

The η-divergence in this equation is written with full ϵ-dependence in terms of a plus distribution with infinity boundary. The plus distributions over a vector domain of the type $\mathcal{L}_n^\beta(\mu, \vec{p}_\perp) \equiv \frac{1}{2\pi\mu^2}\left[\frac{1}{(\vec{p}_\perp^2/\mu^2)^{1+\beta}}\ln^n(\vec{p}_\perp^2/\mu^2)\right]_+^{\mathcal{D}_\mu}$ used in this equation, appear also in the jet broadening case [34] as the integration measure is two-dimensional. They satisfy the condition

$$\int_{\mathcal{D}_\mu} \frac{\mathrm{d}^2\vec{p}_\perp}{(2\pi)^2}\,\mathcal{L}_n^\beta(\mu, \vec{p}_\perp) = 0\,, \tag{4.9}$$

where $\mathcal{D}_\mu$ denotes a disc of radius μ around the origin in the $\vec{p}_\perp$-space. For further details on these distributions we refer to appendix A.2.

4.2 Soft function calculation for $b < 0$

The results for the tree-level and the one-loop soft function given in eqs. (4.1) and (4.2) remain the same for negative-b angularities as well. However, for $b < 0$, the Heaviside

JHEP08(2019)144

θ-function constraint is now equivalent to $\theta(Q\,\tau_R - |\vec{p}_\perp|)$, which leads to the new set of variables

$$u_L = \frac{k_\perp^2}{Q^2\tau_L^2}\,, \qquad u_R = \frac{p_\perp^2}{Q^2\tau_R^2}\,, \tag{4.10}$$

to be used in eq. (4.2) in order to obtain decoupled distributions. This yields

$$\begin{aligned}\mathcal{S}^{(1-)}(\tau_L,\tau_R,\vec{p}_\perp^{\,2},\vec{k}_\perp^{\,2}) &= \mathcal{S}^{(1-)}(\tau_L,\tau_R,u_L,u_R)\left[\left|\frac{\mathrm{d}u_L}{\mathrm{d}k_\perp^2}\right|\left|\frac{\mathrm{d}u_R}{\mathrm{d}p_\perp^2}\right|\right] \\ &= -\frac{\alpha_s(\mu)\,C_F}{\pi}\frac{e^{\epsilon\gamma_E}\,\mu^{2\epsilon}}{\Gamma(1-\epsilon)}\,w^2\nu^\eta\,Q\,\delta(\tau_L)\,\delta(u_L)\,\frac{1}{(Q\tau_R)^{1+2\epsilon+\eta}} \\ &\quad\times\frac{\theta(1-u_R)\,(1-u_R^{-1/b})^{-\eta}}{b\,u_R^{1+\epsilon+\eta/2+\eta/2\,b}}\left[\left|\frac{\mathrm{d}u_L}{\mathrm{d}k_\perp^2}\right|\left|\frac{\mathrm{d}u_R}{\mathrm{d}p_\perp^2}\right|\right] + \left\{\begin{matrix}\tau_L\leftrightarrow\tau_R\\ u_L\leftrightarrow u_R\end{matrix}\right\},\end{aligned} \tag{4.11}$$

where

$$\left|\frac{\mathrm{d}u_L}{\mathrm{d}k_\perp^2}\right| = \frac{1}{Q^2\tau_L^2}\,, \qquad \left|\frac{\mathrm{d}u_R}{\mathrm{d}p_\perp^2}\right| = \frac{1}{Q^2\tau_R^2}\,. \tag{4.12}$$

The numerator term $(1-u_R^{-1/b})^{-\eta}$, like before, does not contribute any singular nor finite term. Moreover, in the present case, all distributions in both $\tau_{L,R}$ and $u_{L,R}$ are already regulated by ϵ. Thus no rapidity divergence is contained in eq. (4.11). Upon expansion of this equation we obtain

$$\begin{aligned}\mathcal{S}^{(1-)}(\tau_L,\tau_R,u_L,u_R) &= \frac{\alpha_s(\mu)\,C_F}{\pi}\,\delta(\tau_L)\,\delta(u_L)\left\{-\frac{1}{2\,b\epsilon^2}\delta(\tau_R)\delta(u_R)+\frac{1}{2b\epsilon}\left[\frac{\theta(1-u_R)}{u_R}\right]_+\delta(\tau_R)\right. \\ &+\frac{1}{b\,\epsilon}\delta(u_R)\frac{Q}{\mu}\left[\frac{1}{Q\,\tau_R/\mu}\right]_+ - \frac{2}{b}\,\delta(u_R)\frac{Q}{\mu}\left[\frac{\ln(Q\,\tau_R/\mu)}{Q\,\tau_R/\mu}\right]_+ - \frac{1}{2\,b}\left[\frac{\theta(1-u_R)\,\ln u_R}{u_R}\right]_+\delta(\tau_R) \\ &\left.-\frac{1}{b}\left[\frac{\theta(1-u_R)}{u_R}\right]_+\frac{Q}{\mu}\left[\frac{1}{Q\,\tau_R/\mu}\right]_+ + \frac{\pi^2}{24\,b}\,\delta(\tau_R)\,\delta(u_R)+\mathcal{O}(\eta,\epsilon)\right\} + \left\{\begin{matrix}\tau_L\leftrightarrow\tau_R\\ u_L\leftrightarrow u_R\end{matrix}\right\}.\end{aligned} \tag{4.13}$$

The absence of rapidity divergences in the soft function is consistent with the fact that the jet function for $b<0$ in eq. (3.16) is also free of rapidity divergences.

4.3 Jet broadening limit of the one-loop soft function

A non-trivial cross-check on our calculation is provided by the fact that we can reproduce the jet broadening soft function by taking the limit $b\to 0$. We will treat the cases $b>0$ and $b<0$ separately after making the suitable change of variable to $v_{L,R}$ and $u_{L,R}$, respectively, and *before* making expansion in η and ϵ.

JHEP08(2019)144

4.3.1 Limit $b \to 0^+$

Since the functional dependence on b is contained only through the redefined variable v_R in eq. (4.4), taking the limit $b \to 0^+$ gives

$$\begin{aligned}\lim_{b\to 0^+} \frac{\theta(1-v_R)\,(1-v_R^{2/b})^{-\eta}}{b\,v_R^{-\eta/b}}\,\frac{1}{v_R}\left|\frac{\mathrm{d}v_R}{\mathrm{d}\tau_R}\right| &= 2\lim_{b\to 0^+}\frac{1}{2\,b}e^{-|\ln(v_R^\eta)|/b}\,\frac{1}{v_R}\left|\frac{\mathrm{d}v_R}{\mathrm{d}\tau_R}\right| \\ &= 2\,\frac{\delta(\ln(v_R^\eta))}{v_R}\left|\frac{\mathrm{d}v_R}{\mathrm{d}\tau_R}\right| \\ &= 2\,Q^2\tau_R\frac{\delta(Q^2\,\tau_R^2-\vec{p}_\perp^{\,2})}{\eta}\left|\frac{\mathrm{d}\tau_R^2}{\mathrm{d}\tau_R}\right|, \end{aligned} \tag{4.14}$$

In the first line of this equation, we have used the fact that $v_R^{2/b} \ll 1$ and $\ln(v_R^\eta) < 0$ for $0 < v_R < 1$ as $b \to 0^+$. Here the factor $\left|\frac{\mathrm{d}\tau_R^2}{\mathrm{d}\tau_R}\right| = 2$ is the Jacobian required for the variable change. The second line of eq. (4.14) follows from

$$\delta(x) = \lim_{\epsilon\to 0}\frac{1}{2\,\epsilon}\,e^{-\frac{|x|}{\epsilon}}\,, \tag{4.15}$$

while in the final step we have used the identity

$$\delta(\ln(v_R^\eta)) = \frac{\delta(v_R-1)}{\eta}\,, \tag{4.16}$$

which when combined with the Jacobian gives a distribution in terms of τ_R and $p_\perp$. Substituting the result of eq. (4.14) in the limit $b \to 0^+$ into eq. (4.4), we get

$$\begin{aligned}\lim_{b\to 0^+}\mathcal{S}^{(1+)}(\tau_L,\tau_R,\vec{p}_\perp^{\,2},\vec{k}_\perp^{\,2}) = \frac{2\,\alpha_s(\mu)\,C_F}{\pi}\frac{w^2\,e^{\epsilon\gamma_E}}{\eta\,\Gamma(1-\epsilon)}\Big(\frac{\mu}{Q}\Big)^{2\epsilon}\Big(\frac{\nu}{Q}\Big)^{\eta}\,\delta(\tau_L)\,\delta(\vec{k}_\perp^{\,2})\,\frac{1}{(\tau_R)^{1+2\epsilon+\eta}} \\ \times\,\delta(Q^2\tau_R^2-\vec{p}_\perp^{\,2}) + \left\{\begin{array}{c}\tau_L\leftrightarrow\tau_R\\ \vec{k}_\perp^{\,2}\leftrightarrow\vec{p}_\perp^{\,2}\end{array}\right\}.\end{aligned} \tag{4.17}$$

After expanding in η and ϵ, this gives

$$\begin{aligned}\lim_{b\to 0^+}\mathcal{S}^{(1+)}(\tau_L,\tau_R,\vec{p}_\perp^{\,2},\vec{k}_\perp^{\,2}) = \frac{\alpha_s(\mu)\,C_F}{\pi}\Bigg\{\frac{2\,w^2e^{\epsilon\gamma_E}}{\eta\,\Gamma(1-\epsilon)}\Big(\frac{\mu}{Q}\Big)^{2\epsilon}\Big[\frac{1}{\tau_R^{1+2\epsilon}}\Big]_+^\infty + \delta(\tau_R)\Big(\frac{1}{2\epsilon^2}-\frac{1}{\epsilon}\ln\frac{\nu}{\mu}\Big) \\ +2\ln\frac{\nu}{\mu}\frac{Q}{\mu}\Big[\frac{\mu}{Q\tau_R}\Big]_+ - \frac{2\,Q}{\mu}\Big[\frac{\mu\ln(Q\tau_R/\mu)}{Q\tau_R}\Big]_+ - \frac{\pi^2}{24}\,\delta(\tau_R)\Bigg\}\delta(\tau_L)\delta(\vec{k}_\perp^{\,2}) \\ \delta(Q^2\tau_R^2-\vec{p}_\perp^{\,2}) + \left\{\begin{array}{c}\tau_L\leftrightarrow\tau_R\\ \vec{k}_\perp^{\,2}\leftrightarrow\vec{p}_\perp^{\,2}\end{array}\right\},\end{aligned} \tag{4.18}$$

which agrees with the one-loop soft function for jet broadening in eq. (6.45) of ref. [34].

JHEP08(2019)144

4.3.2 Limit $b \to 0^-$

The $b \to 0^-$ limit can be obtained in an analogous way by writing the distribution in u_R appearing in eq. (4.11) as

$$\lim_{b\to 0^-} \frac{\theta(1-u_R)\,(1-u_R^{-1/b})^{-\eta}}{(-b)\,u_R^{\eta/2\,b}} \frac{1}{(u_R)^{1+\epsilon+\frac{\eta}{2}}} \left|\frac{\mathrm{d}u_R}{\mathrm{d}p_\perp^2}\right| = 2 \lim_{|b|\to 0^+} \frac{1}{2\,|b|} e^{-|\ln(u_R^{\eta/2})|/|b|} \frac{1}{(u_R)^{1+\epsilon+\frac{\eta}{2}}} \left|\frac{\mathrm{d}u_R}{\mathrm{d}p_\perp^2}\right|$$
$$= 2\,\frac{\delta(u_R-1)}{\eta} \left|\frac{\mathrm{d}u_R}{\mathrm{d}p_\perp^2}\right|, \tag{4.19}$$

which leads to the same result as in eqs. (4.17) and (4.18).

5 One-loop angularity distributions from broadening-like factorization

In this section we will present our one-loop results for the angularity cross sections at arbitrary values of b, which we obtain using the jet and soft functions calculated above. We will provide results for positive-b and negative-b angularities separately. We will show that our analytic results correctly reproduce the known one-loop results for thrust, jet broadening and large-b angularities. As claimed earlier in section 2, we will show that, compared to thrust-like analyses of angularity distributions with $0.5 < b < 1$, our results based on broadening-like factorization contain an extra sub-leading singular correction of the type shown in eq. (2.7). Our treatment of the small-b case shows explicitly that our results for the cross section are continuous in the limit $b \to 0$. In addition, we will derive the first analytic results for the recoil-sensitive angularity cross sections for negative values of b.

5.1 One-loop cross section for $b > 0$

We now calculate the separate contributions to the cross section from the one-loop jet function and the one-loop soft function, which we denote by jet_{1+} and soft_{1+}, respectively. To obtain jet_{1+}, we perform a convolution of the one-loop jet function in eq. (3.11) with the tree-level soft function in eq. (4.1) and the tree-level hard function $H^{(0)}(Q;\mu) = 1$, according to the factorization theorem in eq. (2.1). Including the contribution from both right and left hemispheres, we have

$$\frac{\mathrm{jet}_{1+}}{\sigma_0} = \frac{\alpha_s(\mu)\,C_F}{\pi}\,\delta(\tau_L)\Bigg(-\frac{2\,w^2\,e^{\epsilon\gamma_E}}{\eta\,(1+b)\,\Gamma(1-\epsilon)}\left(\frac{\mu}{Q}\right)^{2\epsilon}\left[\frac{1}{\tau_R^{1+\frac{2\epsilon}{1+b}}}\right]_+^\infty + \frac{1}{\epsilon}\,\ln\frac{\nu}{Q}\,\delta(\tau_R) + \frac{3}{4\,\epsilon}\,\delta(\tau_R)$$
$$- \frac{2}{1+b}\,\ln\frac{\nu}{Q}\,\frac{1}{m}\left[\frac{1}{\tau_R/m}\right]_+ - \frac{3}{2\,(1+b)}\,\frac{1}{m}\left[\frac{1}{\tau_R/m}\right]_+ + \mathcal{J}_0^{(+)}(b)\,\delta(\tau_R)\Bigg) + \{\tau_L \leftrightarrow \tau_R\}\,, \tag{5.1}$$

where σ_0 denotes the Born cross section and

$$\mathcal{J}_0^{(+)}(b) \equiv i_a - i_b^{(+)} = \frac{2}{1+b}\left[\frac{1+8\,b}{8} + \frac{\pi^2}{6\,b} - \int_0^1 \mathrm{d}x\,\frac{1-x+x^2/2}{x}\,\ln\left(1+\left(\frac{x}{1-x}\right)^b\right)\right]$$
$$= \frac{2}{1+b}\left[\frac{1+8\,b}{8} + \frac{\pi^2}{12\,b} - \frac{\pi^2}{12}b - \int_0^1 \mathrm{d}x\left(\frac{x}{2}-1\right)\,\ln\left(1+\left(\frac{x}{1-x}\right)^b\right)\right]. \tag{5.2}$$

JHEP08(2019)144

The integral in the second line is finite as $b \to 0$ and will be treated numerically. The singularity due to $1/x$ in the integrand in the first line of eq. (5.2) is regulated when $b > 0$. Here we have used

$$\int_0^1 \mathrm{d}x\, \frac{1}{x}\, \ln\left(1+\left(\frac{x}{1-x}\right)^b\right) = \frac{\pi^2}{12\,b} + \frac{\pi^2}{12} b\,, \tag{5.3}$$

to obtain the expression given in the second line. The last equation can be easily checked numerically.

Similarly, soft_{1+} is obtained by doing a convolution of the one-loop soft function in eq. (4.8) with the hard and the jet functions at tree level, leading to

$$\begin{aligned}\frac{\mathrm{soft}_{1+}}{\sigma_0} = \frac{\alpha_s(\mu)\, C_F}{\pi}\, \delta(\tau_L) \Bigg(& \frac{2\, w^2\, e^{\epsilon\gamma_E}}{\eta\,(1+b)\,\Gamma(1-\epsilon)} \left(\frac{\mu}{Q}\right)^{2\epsilon} \left[\frac{1}{\tau_R^{1+\frac{2\epsilon}{1+b}}}\right]_+^{\infty} + \frac{1}{2\,\epsilon^2}\,\delta(\tau_R) - \frac{1}{\epsilon}\ln\frac{\nu}{\mu}\,\delta(\tau_R) \\ & - \frac{2}{(1+b)^2\, m}\left[\frac{\ln(\tau_R/m)}{\tau_R/m}\right]_+ + 2\ln\frac{\nu}{\mu}\,\frac{1}{(1+b)\,m}\left[\frac{1}{\tau_R/m}\right]_+ - \frac{\pi^2}{24}\,\delta(\tau_R) + \mathrm{I}_s^{(+)}(\tau_R)\Bigg) \\ & + \{\tau_L \leftrightarrow \tau_R\}\,,\end{aligned} \tag{5.4}$$

where

$$\mathrm{I}_s^{(+)}(\tau_R) = \frac{2}{b}\int_0^{Q\,\tau_R^{1/(1+b)}} \mathrm{d}p_\perp\, \theta\!\left(\frac{p_\perp}{Q} - \tau_R + \left(\frac{p_\perp}{Q}\right)^{1+b}\right) \frac{Q}{p_\perp}\,\frac{1}{\mu}\left[\frac{1}{p_\perp/\mu}\right]_+ \left[\frac{p_\perp/Q}{\tau_R - \left(\frac{p_\perp}{Q}\right)^{1+b}}\right]_+ . \tag{5.5}$$

Writing the integral in the last equation in terms of dimensionless quantities, ρ and τ_R, with

$$\rho \equiv \left(\frac{p_\perp}{Q}\right)^{1+b}, \tag{5.6}$$

we get

$$\mathrm{I}_s^{(+)}(\tau_R) = \frac{2}{b\,(1+b)}\int_{r\,\tau_R}^{\tau_R} \mathrm{d}\rho\, \frac{1}{\rho}\,\frac{Q}{\mu}\left[\frac{\mu/Q}{\rho^{\frac{1}{1+b}}}\right]_+ \left[\frac{\rho^{\frac{1}{1+b}}}{\tau_R - \rho}\right]_+ . \tag{5.7}$$

Here r in the lower limit of integration, $r\,\tau_R$, is obtained by solving the constraint equation

$$\frac{r}{(1-r)^{1+b}} = \tau_R^b\,, \tag{5.8}$$

which stems from the Heaviside θ-function in eq. (5.5) and makes one of the plus prescriptions superfluous. The details of the calculation of the integral $\mathrm{I}_s^{(+)}(\tau_R)$ can be found in appendix D.1. Our final result amounts to

$$\mathrm{I}_s^{(+)}(\tau_R) = -\frac{2\,b}{(1+b)^2}\left[\frac{\ln\tau_R}{\tau_R}\right]_+ - \frac{\pi^2}{3\,b(1+b)}\delta(\tau_R) - \frac{2}{1+b}\frac{\ln(1-r)}{\tau_R}\,. \tag{5.9}$$

Note that in the small-τ_R limit we have $r \sim \tau_R^b$, which implies that the last term is less singular compared to $1/\tau_R$ and thus does not require a plus prescription, unless b is vanishingly small. Since b regulates the small-τ_R limit in the last term, for vanishingly small b the last term needs to be expressed as a distribution as shown in appendix E.1.2.

JHEP08(2019)144

Finally, according to eq. (2.4), the remaining contribution to the one-loop normalized cross section due to the one-loop hard function is

$$\frac{\text{hard}_1}{\sigma_0} = \frac{\alpha_s(\mu)\, C_F}{2\pi}\left(-\frac{1}{\epsilon^2}-\frac{2}{\epsilon}\ln\frac{\mu}{Q}-\frac{3}{2\,\epsilon}-2\ln^2\frac{\mu}{Q}-3\ln\frac{\mu}{Q}-4+\frac{7\pi^2}{12}\right)\delta(\tau_L)\,\delta(\tau_R)+\{\tau_L\leftrightarrow\tau_R\}\ . \tag{5.10}$$

Adding the terms jet_{1+}, soft_{1+} and hard_1, we obtain the $\mathcal{O}(\alpha_s)$ contribution to the double-differential angularity cross section in SCET_{II},

$$\begin{aligned}\left[\frac{1}{\sigma_0}\frac{\mathrm{d}^2\sigma^{(+)}}{\mathrm{d}\tau_L\,\mathrm{d}\tau_R}\right]^{\mathcal{O}(\alpha_s)}_{\text{SCET}_{\text{II}}} &= \frac{\alpha_s(\mu)\, C_F}{\pi}\,\delta(\tau_L)\left[\delta(\tau_R)\left(-2+\frac{\pi^2}{4}-\frac{\pi^2}{3\,b(1+b)}+\mathcal{J}_0^{(+)}(b)\right)\right.\\ &\left.-\frac{3}{2(1+b)}\left[\frac{1}{\tau_R}\right]_+-\frac{2}{(1+b)}\left[\frac{\ln\tau_R}{\tau_R}\right]_+-\frac{2}{1+b}\frac{\ln(1-r)}{\tau_R}\right]+\{\tau_L\leftrightarrow\tau_R\}\ .\end{aligned} \tag{5.11}$$

Notice that the rapidity divergences, identified by $1/\eta$ factors, as well as the ν-dependence cancel out in the sum of the jet and soft contributions, as expected. The ϵ-divergent structure in the sum of jet_{1+} and soft_{1+} is proportional to $\delta(\tau_L)\,\delta(\tau_R)$ and cancels exactly against the ϵ divergences of the hard_1-term, leaving the cross section independent of the choice of regulators and scales, up to a residual dependence on μ through the renormalized coupling $\alpha_s(\mu)$.

Eq. (5.11) serves as the master formula for positive-b angularities and, as we are going to show in the following two subsections, it yields the known expressions for broadening, thrust and large-b angularities in suitable limits.

5.1.1 Small-τ limit

When b is away from 0, the general solution of eq. (5.8) in the small-τ limit can be found as detailed in appendix E.1.1. The double-differential $\mathcal{O}(\alpha_s)$ cross section in the small-τ limit is then given as

$$\begin{aligned}\left[\frac{1}{\sigma_0}\frac{\mathrm{d}^2\sigma^{(+)}}{\mathrm{d}\tau_L\mathrm{d}\tau_R}\right]^{\mathcal{O}(\alpha_s)}_{\text{SCET}_{\text{II}}} &= \frac{\alpha_s(\mu)\, C_F}{\pi}\,\delta(\tau_L)\left[\delta(\tau_R)\left(-2+\frac{\pi^2}{4}-\frac{\pi^2}{3b(1+b)}+\mathcal{J}_0^{(+)}(b)\right)-\frac{3}{2(1+b)}\left[\frac{1}{\tau_R}\right]_+\right.\\ &\left.-\frac{2}{1+b}\left[\frac{\ln\tau_R}{\tau_R}\right]_+-\frac{2}{1+b}\sum_{n=1}^{\lceil 1/b\rceil-1}\frac{c_n}{\tau_R^{1-n\,b}}\right]+\{\tau_L\leftrightarrow\tau_R\}+\text{power corrections},\end{aligned} \tag{5.12}$$

with $\mathcal{J}_0^{(+)}(b)$ as in eq. (5.2) and c_n depending only on b. The first few coefficients appearing in the last equation are given by

$$\begin{aligned}&\mathrm{c}_1=-1, \qquad \mathrm{c}_2=\frac{1}{2}(1+2\,b), \qquad \mathrm{c}_3=-\frac{1}{6}(2+9\,b+9\,b^2),\\ &\mathrm{c}_4=\frac{1}{12}(3+22\,b+48\,b^2+32\,b^3), \quad \mathrm{c}_5=-\frac{1}{120}(24+250\,b+875\,b^2+1250\,b^3+625\,b^4),\ \ldots\ .\end{aligned} \tag{5.13}$$

The result in eq. (5.12) has the structure presented in section 2. For any given (positive) value of b, there exists an integer $N=\lceil 1/b\rceil-1$, up to which terms under the summation

JHEP08(2019)144

contribute as sub-leading singularities. For $n > N$, the recoil effects accounted for by SCET_{II} factorization amount only to power corrections. The other terms agree with the SCET_{I} factorization result.

As discussed earlier in section 2, although the jet function in section 3 and the soft function in section 4 are homogenous in the power counting, the cross section in eq. (5.12) obtained after the transverse momentum convolution contains sub-leading terms that are not, since the transverse momenta scale differently in the jet and the soft sectors. While the new terms are formally sub-leading, their numerical effects can be significant though. Table 1 of section 6 shows the numerical size of these sub-leading singular contributions relative to the leading singular ones, for several values of b.

Using the result in eq. (5.12), we obtain the singular contribution to the one-loop single-differential angularity cross section for $b > 0$, by integrating over the hemisphere angularities subject to the constraint $\tau = \tau_L + \tau_R$,

$$\left[\frac{1}{\sigma_0}\frac{\mathrm{d}\sigma^{(+)}}{\mathrm{d}\tau}\right]^{\mathcal{O}(\alpha_s)}_{\text{sing.}} = \frac{\alpha_s(\mu)\,C_F}{\pi}\left\{-\frac{3}{(1+b)}\left[\frac{1}{\tau}\right]_+ - \frac{4}{1+b}\left[\frac{\ln\tau}{\tau}\right]_+ - \frac{4}{1+b}\sum_{n=1}^{\lceil 1/b\rceil-1}\frac{c_n}{\tau^{1-n\,b}}\right.$$
$$\left. + \delta(\tau)\left[-\frac{7}{2(1+b)} + \frac{\pi^2}{6\,b}\,\frac{b^2+3\,b-2}{1+b} - \frac{4}{1+b}\int_0^1 \mathrm{d}x\left(\frac{x}{2}-1\right)\ln\left(1+\left(\frac{x}{1-x}\right)^b\right)\right]\right\}. \tag{5.14}$$

Here the first two terms as well as the coefficient of $\delta(\tau)$-piece agree with the $\mathcal{O}(\alpha_s)$-singular cross section obtained from SCET_{I} thrust-like factorization in ref. [15]. The terms in the summation are singular only when $0 < b < 1$. When $b \geq 1$, recoil effects amount to regular terms, which can be dropped to obtain the result in [15]. By taking the limit $b \to 1$ in eq. (5.14) and neglecting power corrections, we obtain the $\mathcal{O}(\alpha_s)$-singular thrust distribution

$$\left[\frac{1}{\sigma_0}\frac{\mathrm{d}\sigma^{(+)}}{\mathrm{d}\tau}\right]^{\mathcal{O}(\alpha_s)}_{\text{sing.}} = \frac{\alpha_s(\mu)\,C_F}{\pi}\left[\delta(\tau)\left(-\frac{1}{2}+\frac{\pi^2}{6}\right) - \frac{3}{2}\left[\frac{\theta(\tau)}{\tau}\right]_+ - 2\left[\frac{\theta(\tau)\ln\tau}{\tau}\right]_+\right], \tag{5.15}$$

which agrees with the known result in the literature (see e.g. eq. (36.8) of [48]).

5.1.2 Small-b and the jet broadening limit

In the last term of the master formula in eq. (5.11), the limit $\tau \to 0$ is regulated by the angularity exponent b, implying that the small-b limit requires special care. While b and τ can be small, τ^b need not be small. Thus in this case we need an expansion of r in small b while treating $\tau^b \sim 1$. This is worked out in appendix E.1.2. Using the result in eq. (E.4), we get, for the last term of eq. (5.11),

$$\frac{\ln(1-r)}{\tau_R} = \left(-\frac{\pi^2}{12\,b} + \frac{\ln^2 2}{2} - \frac{b}{4}\ln^2 2\right)\delta(\tau_R) - \ln 2\left[\frac{1}{\tau_R}\right]_+ - \frac{b}{2}\left[\frac{\ln\tau_R}{\tau_R}\right]_+ + \frac{b}{2}\ln 2\left[\frac{1}{\tau_R}\right]_+ + \mathcal{O}(b^2)\,. \tag{5.16}$$

JHEP08(2019)144

The double-differential $\mathcal{O}(\alpha_s)$ cross section, in this limit, up to order b^2 is thus given as

$$\begin{aligned}\left[\frac{1}{\sigma_0}\frac{\mathrm{d}^2\sigma^{(+)}}{\mathrm{d}\tau_L\,\mathrm{d}\tau_R}\right]^{\mathcal{O}(\alpha_s)}_{\mathrm{SCET_{II}}} &= \frac{\alpha_s(\mu)\,C_F}{\pi}\,\delta(\tau_L) \\ &\times\Bigg[\delta(\tau_R)\Bigg(-\frac{\pi^2}{6\,b}+\frac{5\pi^2}{12}-2-\ln^2 2-\frac{\pi^2\,b}{6}+\frac{3\,b}{2}\ln^2 2+\mathcal{J}_0^{(+)}(b)\Bigg) \\ &-\frac{3}{2}\left[\frac{1}{\tau_R}\right]_+-2\left[\frac{\ln\tau_R}{\tau_R}\right]_++2\ln 2\left[\frac{1}{\tau_R}\right]_++b\Bigg(\frac{3}{2}\left[\frac{1}{\tau_R}\right]_++3\left[\frac{\ln\tau_R}{\tau_R}\right]_+-3\ln 2\left[\frac{1}{\tau_R}\right]_+\Bigg)\Bigg] \\ &+\mathcal{O}(b^2)+\{\tau_L\leftrightarrow\tau_R\}\,.\end{aligned} \tag{5.17}$$

The jet convolution factor $\mathcal{J}_0^{(+)}$ (see eq. (5.2)), in the small-b limit, amounts to

$$\mathcal{J}_0^{(+)}(b)=\frac{\pi^2}{6\,b}-\frac{\pi^2}{6}+\frac{1}{4}+\frac{3}{2}\ln 2-b\left(\frac{3}{2}\ln 2-\frac{3}{2}\right)+\mathcal{O}(b^2)\,. \tag{5.18}$$

It is clear from eqs. (5.17) and (5.18) that the $1/b$ singularities cancel, yielding a smooth behavior for the cross section for vanishingly small positive values of b. To order b^2, we have

$$\begin{aligned}\left[\frac{1}{\sigma_0}\frac{\mathrm{d}^2\sigma^{(+)}}{\mathrm{d}\tau_L\,\mathrm{d}\tau_R}\right]^{\mathcal{O}(\alpha_s)}_{\mathrm{SCET_{II}}} &= \frac{\alpha_s(\mu)\,C_F}{\pi}\,\delta(\tau_L) \\ &\times\Bigg[\delta(\tau_R)\Bigg(-\frac{7}{4}+\frac{\pi^2}{4}+\frac{3}{2}\ln 2-\ln^2 2+b\Bigg(-\frac{\pi^2}{6}-\frac{3\ln 2}{2}+\frac{3}{2}+\frac{3\ln^2 2}{2}\Bigg)\Bigg) \\ &-\frac{3}{2}\left[\frac{1}{\tau_R}\right]_+-2\left[\frac{\ln\tau_R}{\tau_R}\right]_++2\ln 2\left[\frac{1}{\tau_R}\right]_++b\Bigg(\frac{3}{2}\left[\frac{1}{\tau_R}\right]_++3\left[\frac{\ln\tau_R}{\tau_R}\right]_+-3\ln 2\left[\frac{1}{\tau_R}\right]_+\Bigg)\Bigg] \\ &+\mathcal{O}(b^2)+\{\tau_L\leftrightarrow\tau_R\}\,.\end{aligned} \tag{5.19}$$

Taking the $b\to 0^+$ limit of the last equation gives

$$\begin{aligned}\left[\frac{1}{\sigma_0}\frac{\mathrm{d}^2\sigma^{(+)}}{\mathrm{d}\tau_L\mathrm{d}\tau_R}\right]^{\mathcal{O}(\alpha_s)}_{\mathrm{sing.}} &= \frac{\alpha_s(\mu)C_F}{\pi}\Bigg\{\delta(\tau_R)\,\delta(\tau_L)\Bigg(-\frac{7}{2}+\frac{\pi^2}{2}-3\ln\frac{\mu}{Q}-2\ln^2\frac{\mu}{Q}\Bigg) \\ &+\Bigg[\delta(\tau_L)\Bigg(-\frac{3\,Q}{4\,\mu}\left[\frac{2\,\mu}{Q\tau_R}\right]_+-\frac{Q}{\mu}\left[\frac{2\,\mu}{Q\tau_R}\right]_+\ln\frac{\mu}{Q}-\frac{Q}{\mu}\left[\frac{2\,\mu\ln(Q\tau_R/2\,\mu)}{Q\tau_R}\right]_+\Bigg)+\{\tau_L\leftrightarrow\tau_R\}\Bigg]\Bigg\}\,,\end{aligned} \tag{5.20}$$

which agrees with the double-differential jet broadening distribution obtained in [34].

5.2 One-loop cross section for $b<0$

To obtain the contribution from the one-loop jet function to the cross section for negative-b (jet_{1-}), we convolve our result in eq. (3.16) with the tree-level soft function of eq. (4.1) and the tree-level hard function $H^{(0)}(Q;\mu)=1$,

$$\begin{aligned}\frac{\mathrm{jet}_{1-}}{\sigma_0} &= \frac{\alpha_s(\mu)\,C_F}{\pi}\,\delta(\tau_L)\Bigg(\frac{1+b}{2\,b\,\epsilon^2}\delta(\tau_R)+\frac{3}{4\,\epsilon}\,\delta(\tau_R)-\frac{1}{b\,\epsilon}\frac{1}{m}\left[\frac{1}{\tau_R/m}\right]_+-\frac{3}{2\,(1+b)}\frac{1}{m}\left[\frac{1}{\tau_R/m}\right]_+ \\ &+\frac{2}{b(1+b)}\frac{1}{m}\left[\frac{\ln(\tau_R/m)}{\tau_R/m}\right]_+-\frac{\pi^2}{24}\frac{1+b}{b}\delta(\tau_R)+\mathcal{J}_0^{(-)}(b)\,\delta(\tau_R)\Bigg)+\{\tau_L\leftrightarrow\tau_R\}\,,\end{aligned} \tag{5.21}$$

JHEP08(2019)144

where

$$\mathcal{J}_0^{(-)}(b) \equiv i_a - i_b^{(-)} = \frac{2}{1+b}\left[\frac{1+6\,b}{8} - \frac{\pi^2}{6}\left(\frac{b^2+1}{b}\right) - \int_0^1 \mathrm{d}x\, \frac{1-x+x^2/2}{x} \ln\left(1+\left(\frac{x}{1-x}\right)^{-b}\right)\right]$$
$$= \frac{2}{1+b}\left[\frac{1+6\,b}{8} - \frac{\pi^2}{12\,b} - \frac{\pi^2}{12}\,b - \int_0^1 \mathrm{d}x\left(\frac{x}{2}-1\right) \ln\left(1+\left(\frac{x}{1-x}\right)^{-b}\right)\right]. \tag{5.22}$$

The integral in the first line of eq. (5.22) has the same form as that given in eq. (5.2) but with b replaced by $-b$. The result of eq. (5.3) holds also in the case of negative b, which we have used to obtain the second line of eq. (5.22). Here again the integral in the second line of the last equation is regular in b and can be computed numerically for a given b.

The contribution to soft_{1-} is derived by taking the convolution of the one-loop soft function of eq. (4.13) with the hard and the jet functions at tree level,

$$\frac{\mathrm{soft}_{1-}}{\sigma_0} = \frac{\alpha_s(\mu)\,C_F}{\pi}\,\delta(\tau_L)\Bigg(-\frac{1}{2\,b\epsilon^2}\,\delta(\tau_R) + \frac{1}{b\,\epsilon}\frac{Q}{\mu}\left[\frac{1}{Q\tau_R/\mu}\right]_+ - \frac{2}{b}\frac{Q}{\mu}\left[\frac{\ln(Q\tau_R/\mu)}{Q\tau_R/\mu}\right]_+ + \frac{\pi^2}{24\,b}\delta(\tau_R)$$
$$+\,\mathrm{I}_s^{(-)}(\tau_R)\Bigg) + \{\tau_L \leftrightarrow \tau_R\}\,. \tag{5.23}$$

It is interesting to note that the b-dependent ϵ-divergences in soft_{1-} cancel exactly against jet_{1-}, while the b-independent ϵ-divergences (contained only in jet_{1-}) cancel against hard_1 of eq. (5.10). The integral $\mathrm{I}_s^{(-)}(\tau_R)$ in soft_{1-} is defined as

$$\mathrm{I}_s^{(-)}(\tau_R) = -\frac{2}{b(1+b)}\int_{s\,\tau_R}^{\tau_R} \mathrm{d}\tau_n^s\, \frac{1}{(\tau_n^s)^2}\,\frac{1}{(\tau_R-\tau_n^s)^{\frac{b-1}{1+b}}}\left[\frac{(\tau_n^s)^2}{(\tau_R-\tau_n^s)^{\frac{2}{1+b}}}\right]_+ \frac{Q}{\mu}\left[\frac{1}{Q\tau_n^s/\mu}\right]_+, \tag{5.24}$$

where s in the lower limit of integration, $s\,\tau_R$, satisfies the constraint equation

$$\frac{s}{(1-s)^{\frac{1}{1+b}}} = \tau_R^{-\frac{b}{1+b}}\,. \tag{5.25}$$

We evaluate the integral in eq. (5.24) in a similar manner as discussed for the positive-b case. The details of this calculation are presented in appendix D.2. The final result is given by

$$\mathrm{I}_s^{(-)}(\tau_R) = \frac{2\,b}{(1+b)^2}\left[\frac{\ln\tau_R}{\tau_R}\right]_+ + \frac{\pi^2}{3\,b(1+b)}\delta(\tau_R) - \frac{2}{(1+b)^2}\frac{\ln(1-s)}{\tau_R}\,. \tag{5.26}$$

Interestingly, this result is similar in structure to eq. (5.9) for positive-b, with the last term yielding sub-leading integrable singularities and/or power corrections, depending on the value of b.

Adding the contribution of jet_{1-} and soft_{1-} to hard_1 given in eq. (5.10), the double-differential $\mathcal{O}(\alpha_s)$ cross section for negative-b in $\mathrm{SCET_{II}}$ amounts to

$$\left[\frac{1}{\sigma_0}\frac{\mathrm{d}^2\sigma^{(-)}}{\mathrm{d}\tau_L\,\mathrm{d}\tau_R}\right]^{\mathcal{O}(\alpha_s)}_{\mathrm{SCET_{II}}} \tag{5.27}$$
$$= \frac{\alpha_s(\mu)\,C_F}{\pi}\,\delta(\tau_L)\left[\delta(\tau_R)\left(-2+\frac{\pi^2}{4}+\frac{\pi^2}{3\,b(1+b)}+\mathcal{J}_0^{(-)}(b)\right) - \frac{3}{2(1+b)}\left[\frac{1}{\tau_R}\right]_+\right.$$
$$\left. -\frac{2}{(1+b)^2}\left[\frac{\ln\tau_R}{\tau_R}\right]_+ - \frac{2}{(1+b)^2}\frac{\ln(1-s)}{\tau_R}\right] + \{\tau_L \leftrightarrow \tau_R\}\,,$$

JHEP08(2019)144

where $\mathcal{J}_0^{(-)}$ is given in eq. (5.22). The last equation represents the master formula for our analysis for $-1 < b < 0$ angularity distributions. This novel result of ours compares successfully against the numerical output of EVENT2, as shown in section 6.

5.2.1 Small-τ limit

For b not close to 0, the solution of eq. (5.25) in the small-τ limit can be expanded in powers of $\tau_R^{-\frac{b}{1+b}}$, as exploited in appendix E.2.1. The double-differential $\mathcal{O}(\alpha_s)$ cross section in the small-τ limit is then given as

$$\begin{aligned}
&\left[\frac{1}{\sigma_0}\frac{\mathrm{d}\sigma^{(-)}}{\mathrm{d}\tau_L \mathrm{d}\tau_R}\right]^{\mathcal{O}(\alpha_s)}_{\mathrm{SCET_{II}}} \\
&= \frac{\alpha_s(\mu)\, C_F}{\pi}\,\delta(\tau_L)\left[\delta(\tau_R)\left(-2+\frac{\pi^2}{4}+\frac{\pi^2}{3\,b(1+b)}+\mathcal{J}_0^{(-)}(b)\right)-\frac{3}{2(1+b)}\left[\frac{1}{\tau_R}\right]_+\right. \\
&\quad \left.-\frac{2}{(1+b)^2}\left[\frac{\ln\tau_R}{\tau_R}\right]_+-\frac{2}{(1+b)^2}\sum_{n=1}^{\lceil 1/|b|\rceil-2}\frac{c_n^{'}}{\tau_R^{1+\frac{n\,b}{1+b}}}\right]+\{\tau_L\leftrightarrow\tau_R\}+\text{power corrections}\,,
\end{aligned} \tag{5.28}$$

where $c_n^{'}$ depend only on the value of b. The first few coefficients are

$$\begin{aligned}
&\mathrm{c}_1^{'}=-1, \qquad \mathrm{c}_2^{'}=\frac{1-b}{2(1+b)}, \qquad \mathrm{c}_3^{'}=-\frac{2-5\,b+2\,b^2}{6(1+b)^2}, \\
&\mathrm{c}_4^{'}=\frac{3-13\,b+13\,b^2-3\,b^3}{12(1+b)^3}, \qquad \mathrm{c}_5^{'}=-\frac{24-154\,b+269\,b^2-154\,b^3+24\,b^4}{120(1+b)^4}, \ldots\,.
\end{aligned} \tag{5.29}$$

The summation is truncated up to the greatest integer which is strictly less than $1/|b|-1$ and includes sub-leading singular terms for $b > -0.5$. For $b \leq -0.5$, only power corrections remain. Using this result, the $\mathcal{O}(\alpha_s)$ singular contribution to the single-differential cross section for negative-b is

$$\begin{aligned}
\left[\frac{1}{\sigma_0}\frac{\mathrm{d}\sigma^{(-)}}{\mathrm{d}\tau}\right]^{\mathcal{O}(\alpha_s)}_{\text{sing.}} &= \frac{\alpha_s(\mu)\, C_F}{\pi}\left\{-\frac{3}{1+b}\left[\frac{1}{\tau}\right]_+-\frac{4}{(1+b)^2}\left[\frac{\ln\tau}{\tau}\right]_+-\frac{4}{(1+b)^2}\sum_{n=1}^{\lceil 1/|b|\rceil-2}\frac{c_n^{'}}{\tau^{1+\frac{n\,b}{1+b}}}\right. \\
&\quad \left.+\,\delta(\tau)\left[-\frac{7+2\,b}{2(1+b)}+\frac{\pi^2(b+2)}{6\,b}-\frac{4}{1+b}\int_0^1 \mathrm{d}x\left(\frac{x}{2}-1\right)\ln\left(1+\left(\frac{x}{1-x}\right)^{-b}\right)\right]\right\}.
\end{aligned} \tag{5.30}$$

It is worth to stress that the coefficients of the $[\ln\tau/\tau]_+$ and $\delta(\tau)$ terms in the equation above differ from the corresponding ones in the positive-b case (see eq. (5.14)) while the coefficient of $[1/\tau]_+$ remains the same.

5.2.2 Small-b and the jet broadening limit

As in the case of positive-b angularities, the last term of our master formula in eq. (5.27), needs to be treated with special care when b and τ are both small. This case is analysed in appendix E.2.2. Using eq. (E.12), we get for the last term of eq. (5.27),

$$\begin{aligned}
\frac{\ln(1-s)}{\tau_R} &= \left(\frac{\pi^2}{12\,b}+\frac{\pi^2}{12}+\frac{\ln^2 2}{2}+\frac{b}{4}\ln^2 2\right)\delta(\tau_R) \\
&\quad -\ln 2\left[\frac{1}{\tau_R}\right]_+ +\frac{b}{2}\left[\frac{\ln\tau_R}{\tau_R}\right]_+ -\frac{b}{2}\ln 2\left[\frac{1}{\tau_R}\right]_+ +\mathcal{O}(b^2)\,.
\end{aligned} \tag{5.31}$$

JHEP08(2019)144

For the double-differential cross section for negative, small b, we obtain to order b^2

$$\begin{aligned}\left[\frac{1}{\sigma_0}\frac{\mathrm{d}^2\sigma^{(-)}}{\mathrm{d}\tau_L\,\mathrm{d}\tau_R}\right]^{\mathcal{O}(\alpha_s)}_{\mathrm{SCET_{II}}} &= \frac{\alpha_s(\mu)\,C_F}{\pi}\,\delta(\tau_L) \\ &\times\Bigg[\delta(\tau_R)\left(\frac{\pi^2}{6\,b}+\frac{\pi^2}{12}-2-\ln^2 2+\frac{\pi^2\,b}{6}+\frac{3\,b}{2}\ln^2 2+\mathcal{J}_0^{(-)}(b)\right) \\ &-\frac{3}{2}\left[\frac{1}{\tau_R}\right]_+-2\left[\frac{\ln\tau_R}{\tau_R}\right]_++2\ln 2\left[\frac{1}{\tau_R}\right]_++b\left(\frac{3}{2}\left[\frac{1}{\tau_R}\right]_++3\left[\frac{\ln\tau_R}{\tau_R}\right]_+-3\ln 2\left[\frac{1}{\tau_R}\right]_+\right)\Bigg] \\ &+\mathcal{O}(b^2)+\{\tau_L\leftrightarrow\tau_R\}\,,\end{aligned} \tag{5.32}$$

where jet convolution integral $\mathcal{J}_0^{(-)}$ in eq. (5.22), up to order b^2, is

$$\mathcal{J}_0^{(-)}(b) = -\frac{\pi^2}{6\,b}+\frac{\pi^2}{6}+\frac{1}{4}+\frac{3}{2}\ln 2+b\left(\frac{3}{2}-\frac{\pi^2}{3}-\frac{3}{2}\ln 2\right)+\mathcal{O}(b^2)\,. \tag{5.33}$$

As in the positive-b case, both jet and soft terms contain $1/b$ singularities which cancel out in the cross section, leading to

$$\begin{aligned}\left[\frac{1}{\sigma_0}\frac{\mathrm{d}^2\sigma^{(-)}}{\mathrm{d}\tau_L\,\mathrm{d}\tau_R}\right]^{\mathcal{O}(\alpha_s)}_{\mathrm{SCET_{II}}} &= \frac{\alpha_s(\mu)\,C_F}{\pi}\,\delta(\tau_L) \\ &\times\Bigg[\delta(\tau_R)\left(-\frac{7}{4}+\frac{\pi^2}{4}-\ln^2 2+\frac{3\ln 2}{2}+b\left(\frac{3}{2}-\frac{\pi^2}{3}-\frac{3\ln 2}{2}+\frac{3\ln^2 2}{2}\right)\right) \\ &-\frac{3}{2}\left[\frac{1}{\tau_R}\right]_+-2\left[\frac{\ln\tau_R}{\tau_R}\right]_++2\ln 2\left[\frac{1}{\tau_R}\right]_++b\left(\frac{3}{2}\left[\frac{1}{\tau_R}\right]_++3\left[\frac{\ln\tau_R}{\tau_R}\right]_+-3\ln 2\left[\frac{1}{\tau_R}\right]_+\right)\Bigg] \\ &+\mathcal{O}(b^2)+\{\tau_L\leftrightarrow\tau_R\}\,.\end{aligned} \tag{5.34}$$

Taking the $b\to 0^-$ limit of this result gives

$$\begin{aligned}\left[\frac{1}{\sigma_0}\frac{\mathrm{d}^2\sigma^{(-)}}{\mathrm{d}\tau_L\mathrm{d}\tau_R}\right]^{\mathcal{O}(\alpha_s)}_{\mathrm{sing.}} &= \frac{\alpha_s(\mu)C_F}{\pi}\Bigg\{\delta(\tau_R)\,\delta(\tau_L)\left(-\frac{7}{2}+\frac{\pi^2}{2}-3\ln\frac{\mu}{Q}-2\ln^2\frac{\mu}{Q}\right) \\ &+\left[\delta(\tau_L)\left(-\frac{3\,Q}{4\,\mu}\left[\frac{2\,\mu}{Q\tau_R}\right]_+-\frac{Q}{\mu}\left[\frac{2\,\mu}{Q\tau_R}\right]_+\ln\frac{\mu}{Q}-\frac{Q}{\mu}\left[\frac{2\,\mu\ln(Q\tau_R/2\,\mu)}{Q\tau_R}\right]_+\right)+\{\tau_L\leftrightarrow\tau_R\}\right]\Bigg\}\,,\end{aligned} \tag{5.35}$$

which agrees with the double-differential jet broadening distribution obtained in [34].

Since its left and the right limits ($b\to 0^\pm$) are the same, our cross section is a continuous function of the angularity parameter at $b=0$. However, it is interesting to note that the soft and the jet functions independently, upon expansion in the regulators, are not smooth functions of b at $b=0$, as in the case of angularities measured with respect to a recoil-insensitive axis [24].

6 Numerical analysis and comparison against Event2

We compare both the broadening-like and the thrust-like normalized single-differential angularity distributions against numerical output from the Event2 generator [49], for six different angularity exponents. In particular, for $b=\{2,1,0.2\}$, we used 10^{12} events from

JHEP08(2019)144

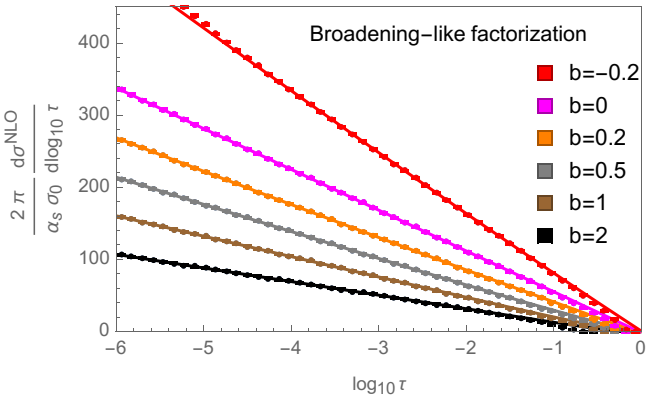

Figure 4. Normalized one-loop angularity cross sections from EVENT2 against our analytic one-loop results based on broadening-like factorization for a variety of exponents.

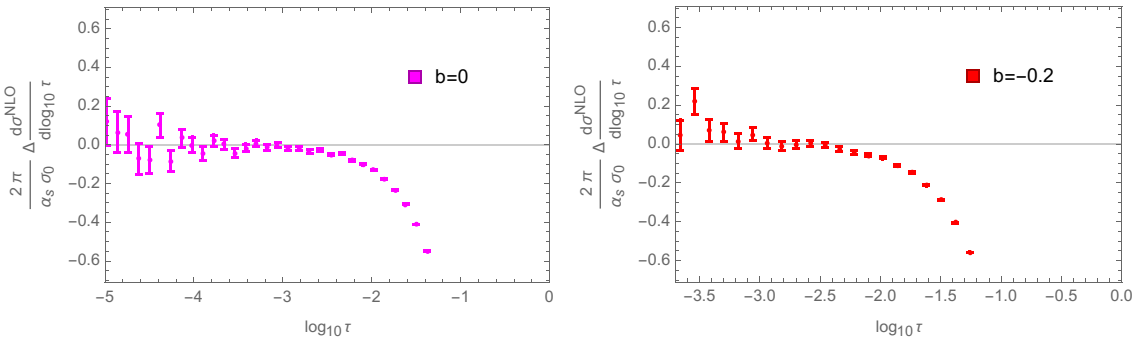

Figure 5. Differences between EVENT2 and our one-loop results from $\mathrm{SCET_{II}}$ factorization for $d\sigma/d\log_{10}\tau$ in the cases of $b = 0$ (jet broadening) and $b = -0.2$.

the runs in [25] with $n_f = 5$, an infrared cutoff $\rho = 10^{-10}$ and, in addition, we generated 10^{11} events with values of ρ as low as 10^{-18} for $b = \{0.5, 0, -0.2\}$.[10]

Figure 4 shows the normalized $d\sigma/d\log_{10}\tau$ distribution from EVENT2 against our analytic one-loop expressions from eq. (5.11) and eq. (5.27), which include both sub-leading singular terms and power corrections due to recoil. Here we use our untruncated results since our power corrections can be large and can significantly contribute to the agreement with EVENT2.

We found agreement within numerical uncertainties between EVENT2 and broadening-like $\mathrm{SCET_{II}}$ factorization for sufficiently small values of τ for all values of b we tested. As an example, the differences between the EVENT2 output and our expressions for $d\sigma/d\log_{10}\tau$ for $b = 0$ (jet broadening case) and $b = -0.2$ are shown in Figure 5 for ranges of τ where no visible cutoff effects are present. The comparison is successful also for the differential cross section $d\sigma/d\tau = 1/(\log_{10}\tau)\, d\sigma/d\log_{10}\tau$, as illustrated in Figure 6 again for $b = 0$ and $b = -0.2$.

[10]The parameter ρ is defined by the fact that EVENT2 regulates infrared divergences by cutting on the invariant mass of pairs of partons, $(p_i + p_j)^2 > \rho\, Q^2$.

JHEP08(2019)144

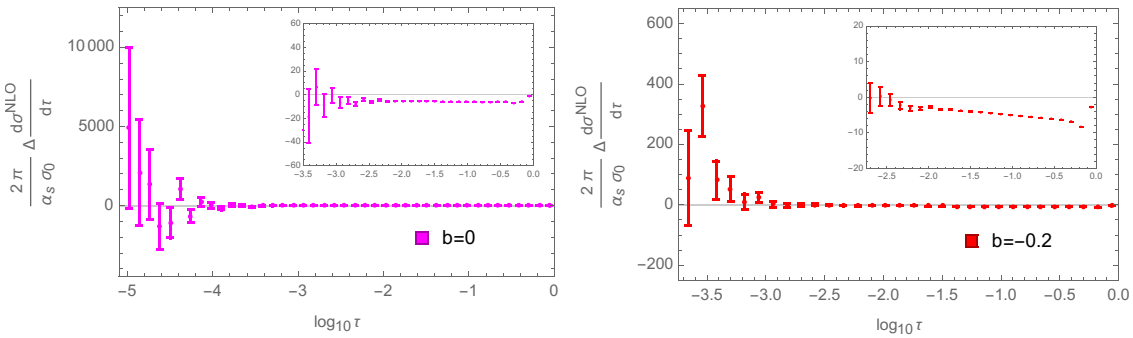

Figure 6. Differences between EVENT2 and our one-loop predictions from $\mathrm{SCET_{II}}$ factorization for $\mathrm{d}\sigma/\mathrm{d}\tau$ for $b = 0$ and $b = -0.2$. The insets magnify the region of larger values of τ.

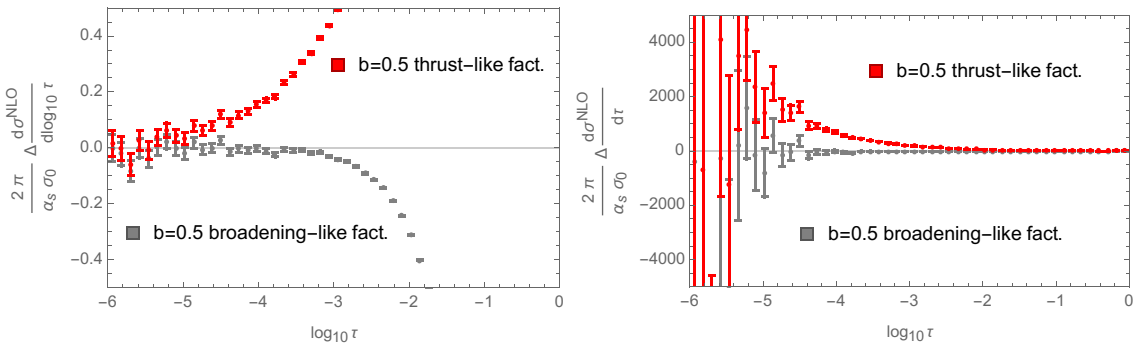

Figure 7. Differences between EVENT2 and thrust-like ($\mathrm{SCET_I}$)/broadening-like ($\mathrm{SCET_{II}}$) one-loop results for $\mathrm{d}\sigma/\mathrm{d}\log_{10}\tau$ (left panel) and $\mathrm{d}\sigma/\mathrm{d}\tau$ (right panel) for $b = 0.5$.

For $b \geq 0.5$, we found agreement within error bars between EVENT2 and both thrust-like and broadening-like factorization for sufficiently small values of τ.[11] Figure 7 illustrates the case of $b = 0.5$, both for $\mathrm{d}\sigma/\mathrm{d}\log_{10}\tau$ and $\mathrm{d}\sigma/\mathrm{d}\tau$. As shown in these plots, the extra terms provided by the $\mathrm{SCET_{II}}$ factorization theorem clearly improve the agreement with EVENT2 in the region of intermediate values of τ.

The relative size of the sum of the sub-leading singular terms compared to the leading singular contribution is shown table 1. Since these contributions turn out to be non-negligible in the peak region also for $0.5 < b < 1$, it is possible that the resummation of these terms plays an important role in precision calculations and extractions of the strong coupling. This will be addressed in a future publication [32].

7 Conclusions

In this paper, we have started to investigate how a theoretical framework based on $\mathrm{SCET_{II}}$ factorization allows us to compute angularity distributions measured with respect to the thrust axis for any value of the exponent b. Working out the analytic expressions of these

[11] The consistency between EVENT2 and thrust-like factorization up to NNLO for $b \geq 0.5$ has been recently discussed and exploited in [22].

JHEP08(2019)144

b	$N = \max(n)$	% correction for $\tau_b = 0.05$	% correction for $\tau_b = 0.1$
1	0	0	0
0.8	1	4	10
0.5	1	10	20
0.25	3	17	30
0	∞	31	45
-0.2	3	16	27
-0.3	2	8	14
-0.5	0	0	0

Table 1. Relative size of the sum of the sub-leading singular terms compared to the leading singular contribution in the peak region for the τ_b distribution, for various values of b, see eq. (5.12) and eq. (5.28). For a given b, N denotes the maximum value of the summation index n up to which the sub-leading terms are singular.

cross sections is a rich and complex problem due to the presence of two kinematic scales ($Q\tau$ and transverse momentum), two types of divergences and renormalization scales, and a continuous dependence of the mode scalings on b, which interpolates between different regimes. As a first step, we have focused on fixed-order calculations, and determined origin and nature of the various divergent structures appearing in the bare angularity jet and soft functions for arbitrary b, which get cancelled in the computation of the cross section. We have produced novel one-loop results for the range $b < 1$, which open up the possibility to use our formalism to extend present analyses of high-precision LEP data. We have computed and numerically quantified previously unknown recoil effects in the perturbative part of the spectrum for all values of b and showed how the known limits of thrust and broadening are reproduced in our framework. All our one-loop distributions are found to be in agreement with Event2 and our $\mathrm{SCET_{II}}$ formalism is shown to capture important sub-leading effects that clearly improve the agreement with Event2 in the region of intermediate values of τ.

Depending on the value of b, recoil effects amount to sub-leading singular terms and/or power corrections in the differential angularity distributions. These singular terms are integrable fractional powers of τ_b and their contribution at fixed-order turns out to be non-negligible even for $b > 0.5$. It will thus be interesting to assess how the resummation of these terms is going to affect precision calculations and the extraction of the strong coupling from data.

Acknowledgments

We thank André Hoang and Wouter Waalewijn for fruitful discussions and for feedback on the manuscript. We thank Wouter Waalewijn for high-statistics Event2 runs on the computer cluster at NIKHEF. We are also grateful to Jui-Yu Chiu, Wouter Waalewijn and Duff Neill for collaboration at an early stage of this work. AJ acknowledges support by a Ramanujan Fellowship of SERB DST. We also thank the Erwin-Schrödinger International Institute for Mathematics and Physics in Vienna for partial support.

JHEP08(2019)144

A Plus distributions and their identities

Here we collect definitions and properties of plus distributions relevant for our calculations.

A.1 Plus distributions over scalar domains

The standard plus distribution with boundary at $x = x_0$ for a function $f(x)$ which is less singular than $1/x^2$ as $x \to 0$, is defined as

$$[\theta(x)\, f(x)]_+^{x=x_0} = \lim_{\epsilon\to 0}[\theta(x-\epsilon)\, f(x) + \delta(x-\epsilon)\, F(x, x_0)]\,, \tag{A.1}$$

with

$$F(x, x_0) = \int_{x_0}^{x} \mathrm{d}x'\, f(x')\,. \tag{A.2}$$

In addition, the distribution satisfies the boundary condition

$$\int_0^{x_0} \mathrm{d}x\, [\theta(x)\, f(x)]_+^{x=x_0} = 0\,. \tag{A.3}$$

Plus distributions with two different boundaries can be related to each other. For boundaries $x = x_0$ and $x = +1$,

$$[\theta(x)\, f(x)]_+^{x=x_0} = [\theta(x)\, f(x)]_+ + \delta(x) \int_{x_0}^{1} \mathrm{d}x'\, f(x')\,. \tag{A.4}$$

In particular, we define the distributions relevant for this work as

$$\mathcal{L}_n^{\beta}(x; x_0) \equiv \left[\frac{\theta(x)}{x^{1+\beta}}\, \ln^n x\right]_+^{x_0}\,, \tag{A.5}$$

so that,

$$\begin{aligned} \mathcal{L}_0^{\beta}(x; 1) = \mathcal{L}^{\beta}(x) &\equiv \left[\frac{\theta(x)}{x^{1+\beta}}\right]_+\,, \\ \mathcal{L}_n^{0}(x; 1) = \mathcal{L}_n(x) &\equiv \left[\frac{\theta(x)}{x}\, \ln^n x\right]_+\,. \end{aligned} \tag{A.6}$$

Note that from the definition above, $\mathcal{L}^0 = \mathcal{L}_0$. The identity in eq. (A.4) for $\mathcal{L}^{\beta}$ and $\mathcal{L}_1^{\beta}$ then gives

$$\mathcal{L}^{\beta}(x; \infty) = -\frac{1}{\beta}\, \delta(x) + \mathcal{L}^0(x) - \beta\, \mathcal{L}_1(x) + \mathcal{O}(\beta^2)\,, \tag{A.7}$$

$$\mathcal{L}_1^{\beta}(x; \infty) = -\frac{1}{\beta^2}\, \delta(x) + \mathcal{L}_1(x) - \beta\, \mathcal{L}_2(x) + \mathcal{O}(\beta^2)\,. \tag{A.8}$$

Another useful property is the rescaling identity (for $\zeta > 0$) for the two special cases above,

$$\mathcal{L}^{\beta=0}(x/\zeta) \equiv \frac{1}{\zeta}\left[\frac{\theta(x)}{x/\zeta}\right]_+ = \mathcal{L}^0(x) - \ln\zeta\, \delta(x)\,, \tag{A.9}$$

$$\mathcal{L}_{n=1}(x/\zeta) \equiv \frac{1}{\zeta}\left[\frac{\theta(x)\ln(x/\zeta)}{x/\zeta}\right]_+ = \mathcal{L}_1(x) - \ln\zeta\, \mathcal{L}^0(x) + \frac{1}{2}\ln^2\zeta\, \delta(x)\,. \tag{A.10}$$

JHEP08(2019)144

A.2 Plus distributions over vector domains

For the class of vector distributions of the type [34]

$$\mathcal{L}_n^\beta(\mu,\vec{p}_\perp) \equiv \frac{1}{2\pi\mu^2}\left[\frac{1}{(\vec{p}_\perp^2/\mu^2)^{1+\beta}}\ln^n(\vec{p}_\perp^2/\mu^2)\right]_+^{\mathcal{D}_\mu}, \tag{A.11}$$

used in eq. (4.8), we define two limiting cases:

$$\mathcal{L}_0^\beta(\mu,\vec{p}_\perp) = \mathcal{L}^\beta(\mu,\vec{p}_\perp) \equiv \frac{1}{2\pi\mu^2}\left[\frac{1}{(\vec{p}_\perp^2/\mu^2)^{1+\beta}}\right]_+^{\mathcal{D}_\mu}, \tag{A.12}$$

$$\mathcal{L}_n^0(\mu,\vec{p}_\perp) = \mathcal{L}_n(\mu,\vec{p}_\perp) \equiv \frac{1}{2\pi\mu^2}\left[\frac{\ln^n(\vec{p}_\perp^2/\mu^2)}{(\vec{p}_\perp^2/\mu^2)}\right]_+^{\mathcal{D}_\mu}. \tag{A.13}$$

Here $\mathcal{D}_\mu$ denotes a disc of radius μ about the origin in the $\vec{p}_\perp$-space. The plus distribution $\mathcal{L}_n^\beta(\mu,\vec{p}_\perp)$ over a vector function is then defined as

$$\int\frac{\mathrm{d}^2\vec{p}_\perp}{(2\pi)^2}\,g(\vec{p}_\perp)\mathcal{L}_n^\beta(\mu,\vec{p}_\perp) = \lim_{\epsilon\to0^+}\frac{1}{2\pi}\int\frac{\mathrm{d}^{2+2\epsilon}\vec{p}_\perp}{(2\pi)^{2+2\epsilon}}\,g(\vec{p}_\perp)\frac{1}{\mu^{2+2\epsilon}}\frac{\ln^n(\vec{p}_\perp^2/\mu^2)}{(\vec{p}_\perp^2/\mu^2)^{1+\beta}} - \frac{g(0)}{2\pi}B_\epsilon[f;\mu], \tag{A.14}$$

where, $g(\vec{p}_\perp)$ is a suitably chosen test function that has no singularities at the origin. The boundary term, B_ϵ, defined as

$$B_\epsilon[\mathcal{L}_n^\beta;\mu] = \frac{1}{2\pi}\int_{\mathcal{D}_\mu}\frac{\mathrm{d}^{2+2\epsilon}\vec{q}_\perp}{(2\pi)^{2+2\epsilon}}\frac{1}{\mu^{2+2\epsilon}}\frac{\ln^n(\vec{q}_\perp^2/\mu^2)}{(\vec{q}_\perp^2/\mu^2)^{1+\beta}}, \tag{A.15}$$

is such that the condition

$$\int_{\mathcal{D}_\mu}\frac{\mathrm{d}^2\vec{q}_\perp}{(2\pi)^2}\,\mathcal{L}_n^\beta(\mu,\vec{q}_\perp) = 0 \tag{A.16}$$

is satisfied. The explicit expression for the boundary term, in dimensional regularization, for the distributions $\mathcal{L}^\beta$ and $\mathcal{L}_n$, is given as

$$B_\epsilon[\mathcal{L}^\beta;\mu] = \frac{1}{(4\pi)^{1+\epsilon}\,\Gamma(1+\epsilon)\,(\epsilon-\beta)}, \tag{A.17}$$

$$B_\epsilon[\mathcal{L}_n;\mu] = \frac{(-1)^n\,\Gamma(1+n)}{(4\pi)^{1+\epsilon}\,\Gamma(1+\epsilon)\,\epsilon^{1+n}}. \tag{A.18}$$

For completeness, we also mention the rescaling identities ($\rho > 0$),

$$\mathcal{L}^\beta\Big(\rho\mu,\vec{p}_\perp\Big) = \rho^{2\beta}\mathcal{L}^\beta\Big(\mu,\vec{p}_\perp\Big) - \frac{\rho^{2\beta}-1}{2\,\beta}\,\delta^{(2)}(\vec{p}_\perp), \tag{A.19}$$

$$\mathcal{L}_n\Big(\rho\mu,\vec{p}_\perp\Big) = \sum_{m=0}^{n}{}_nC_m\,(-1)^{n-m}\ln^m(\rho^2)\mathcal{L}_{n-m}\Big(\mu,\vec{p}_\perp\Big) - \frac{\ln^{n+1}(\rho^2)}{2(n+1)}\,\delta^{(2)}(\vec{p}_\perp), \tag{A.20}$$

with ${}_nC_m = \Gamma(1+n)/[\Gamma(1+m)\Gamma(1+n-m)]$.

JHEP08(2019)144

B Evaluation of the one-loop jet function

In this appendix, we present the details of the calculation for the jet function diagrams and the relevant zero-bin subtractions for all $b > -1$ angularities.

B.1 Jet diagram (a)

Since the jet diagram (a) in Figure 2 contains no rapidity divergence, the η-regulator can be dropped. The diagram in Feynman gauge is then given as

$$
\begin{aligned}
&\mathcal{J}_{\mathrm{a}}^{(1)}(\tau_R, 0) \\
&= \left(\frac{e^{\gamma_E}\mu^2}{4\pi}\right)^{\epsilon} \frac{(2\pi)^{3-2\epsilon}}{N_c} \int \frac{\mathrm{d}^d l}{(2\pi)^{d-1}}\, \delta(l^2)\, \theta(l^0) \int \frac{\mathrm{d}^d p}{(2\pi)^{d-1}}\, \delta(p^2)\, \theta(p^0)\, \delta(p^- + l^- - Q) \\
&\quad \times \delta^{d-2}(\vec{l}_\perp + \vec{p}_\perp)\, \delta\!\left(\tau_R - \frac{|\vec{p}_\perp|}{Q}\left(\frac{p^+}{p^-}\right)^{\frac{b}{2}} - \frac{|\vec{l}_\perp|}{Q}\left(\frac{l^+}{l^-}\right)^{\frac{b}{2}}\right) \mathrm{tr}\left[\frac{\bar{\not{n}}}{2}\, \frac{i(\not{l} + \not{p})}{(l+p)^2}\, (ig\,\gamma^\mu T^a)\right. \\
&\quad \left. \times\, u_s(p)\, \bar{u}_s(p)\, (-g_{\mu\nu})\, (ig\,\gamma^\nu T^a)\, \frac{i(\not{l} + \not{p})}{(l+p)^2}\right] \\
&= -\frac{\alpha_s(\mu)\, C_F}{2\pi^{2-\epsilon}} e^{\epsilon\gamma_E} \mu^{2\epsilon} \int \mathrm{d}^d l\, \delta(l^2)\, \theta(l^0) \int \mathrm{d}^d p\, \delta(p^2)\, \theta(p^0)\, \delta(p^- + l^- - Q)\, \delta^{(d-2)}(\vec{l}_\perp + \vec{p}_\perp) \\
&\quad \times \delta\!\left(\tau_R - \frac{|\vec{p}_\perp|}{Q}\left(\frac{p^+}{p^-}\right)^{\frac{b}{2}} - \frac{|\vec{l}_\perp|}{Q}\left(\frac{l^+}{l^-}\right)^{\frac{b}{2}}\right) \mathrm{tr}\left[\frac{\bar{\not{n}}}{2}\, \frac{(\not{l} + \not{p})}{(l+p)^2}\, \gamma^\mu\, \not{p}\, \gamma_\mu\, \frac{(\not{l} + \not{p})}{(l+p)^2}\right] \\
&= \frac{\alpha_s(\mu) C_F}{\pi}\, \frac{e^{\epsilon\gamma_E}}{\Gamma(1-\epsilon)} \left(\frac{\mu}{Q}\right)^{2\epsilon} \frac{1}{\tau_R^{1+\frac{2\epsilon}{1+b}}}\, \frac{1-\epsilon}{1+b} \int_0^1 \mathrm{d}x\, x\, \left((1-x)^{-b} + x^{-b}\right)^{\frac{2\epsilon}{1+b}}\,.
\end{aligned}
\tag{B.1}
$$

Here $x = l^-/Q$ is the light-cone momentum fraction of the emitted gluon. The trace in the second line of the integral simplifies as follows

$$
\begin{aligned}
\mathrm{tr}\left[\frac{\bar{\not{n}}}{2}\, \frac{(\not{l} + \not{p})}{(l+p)^2}\, \gamma^\mu\, \not{p}\, \gamma_\mu\, \frac{(\not{l} + \not{p})}{(l+p)^2}\right] &= (2-d)\mathrm{tr}\left[\frac{\bar{\not{n}}}{2}\, (\not{l} + \not{p})\, \not{p}\, (\not{l} + \not{p})\right] \times \frac{1}{[(l+p)^2 + i\epsilon]^2} \\
&= (2-d)\, p^+\, \frac{(l^- + p^-)^2}{[(l+p)^2 + i\epsilon]^2} \times \mathrm{tr}\left[\frac{\bar{\not{n}}}{2}\, \frac{\not{n}}{2}\, \frac{\bar{\not{n}}}{2}\, \frac{\not{n}}{2}\right] \\
&= -2(1-\epsilon)\, \frac{p^+}{(l^+ + p^+)^2} \times 2\,,
\end{aligned}
\tag{B.2}
$$

and the final result is obtained by performing the delta function integrals. The analytical expression of the integral in the last line of eq. (B.1) is not known. However, the divergence structure of interest can be obtained by expanding the result of eq. (B.1) in powers of ϵ. The result, upon expansion, is given as

$$
\mathcal{J}_{\mathrm{a}}^{(1)}(\tau_R, 0) = \frac{\alpha_s(\mu) C_F}{\pi} \left[-\frac{1}{4\,\epsilon}\, \delta(\tau_R) + \frac{1}{2(1+b)}\, \mathcal{L}^0\!\left(\frac{\tau_R}{m}\right) + i_a\, \delta(\tau_R) + \mathcal{O}(\epsilon)\right], \tag{B.3}
$$

where

$$
i_a = \frac{1}{4(1+b)} - \frac{1}{1+b} \int_0^1 \mathrm{d}x\, x\, \ln\!\left(1 + \left(\frac{x}{1-x}\right)^b\right), \tag{B.4}
$$

and $m = (\mu/Q)^{1+b}$, is a scale factor. The same result holds for negative-b angularities as well.

JHEP08(2019)144

B.2 Jet diagram (b)

The jet diagram (b), in general, contains rapidity divergences for both the unsubtracted jet integral and its corresponding zero-bin contribution. However, as discussed in the text, the net result of the jet diagram (b), i.e. $\mathcal{J}_{\text{b,unsub}} - \mathcal{J}_{b,0}$, contains no rapidity divergence for $-1 < b < 0$. Here we will present the calculation of the unsubtracted diagram separately for positive-b and negative-b cases. The zero-bin contribution is evaluated in appendix B.3.

B.2.1 Positive-b angularities

The Feynman integral for the unsubtracted jet diagram (b) and its mirror image, is given as

$$
\begin{aligned}
&\mathcal{J}^{(1+)}_{\text{b,unsub}}(\tau_R, 0) \\
&= 2\left(\frac{e^{\gamma_E}\mu^2}{4\pi}\right)^{\epsilon} \frac{(2\pi)^{3-2\epsilon}}{N_c} \int \frac{\mathrm{d}^d l}{(2\pi)^{d-1}}\, \delta(l^2)\, \theta(l^0) \int \frac{\mathrm{d}^d p}{(2\pi)^{d-1}}\, \delta(p^2)\, \theta(p^0)\, \delta(p^- + l^- - Q) \\
&\quad \times \delta\!\left(\tau_R - \frac{|\vec{p}_\perp|}{Q}\left(\frac{p^+}{p^-}\right)^{\frac{b}{2}} - \frac{|\vec{l}_\perp|}{Q}\left(\frac{l^+}{l^-}\right)^{\frac{b}{2}}\right) \delta^{d-2}(\vec{l}_\perp + \vec{p}_\perp)\, \mathrm{tr}\Bigg[\frac{\bar{\not{n}}}{2}\, \frac{i(\not{l} + \not{p})}{(l+p)^2}\, (ig\,\gamma^\mu T^a) \\
&\quad \times u_s(p)\, \bar{u}_s(p)\, (-g_{\mu\nu}) \frac{(g\,\bar{n}^\nu T^a\, \nu^\eta w^2)}{(\bar{n}\cdot l)^{1+\eta}}\Bigg] \\
&= \frac{2}{1+b}\, \frac{\alpha_s(\mu) C_F}{\pi}\, \frac{e^{\epsilon\gamma_E} w^2}{\Gamma(1-\epsilon)} \left(\frac{\mu}{Q}\right)^{2\epsilon} \left(\frac{\nu}{Q}\right)^{\eta} \frac{1}{\tau_R^{1+\frac{2\epsilon}{1+b}}} \int_0^1 \mathrm{d}x\, ((1-x)^{-b} + x^{-b})^{\frac{2\epsilon}{1+b}}\, \frac{(1-x)}{x^{1+\eta}} \\
&= \frac{2}{1+b}\, \frac{\alpha_s(\mu) C_F}{\pi}\, \frac{e^{\epsilon\gamma_E} w^2}{\Gamma(1-\epsilon)} \left(\frac{\mu}{Q}\right)^{2\epsilon} \left(\frac{\nu}{Q}\right)^{\eta} \frac{1}{\tau_R^{1+\frac{2\epsilon}{1+b}}} \int_0^1 \mathrm{d}x \left(1 + \left(\frac{x}{1-x}\right)^b\right)^{\frac{2\epsilon}{1+b}} \frac{(1-x)}{x^{1+\eta+\frac{2\epsilon\, b}{1+b}}}. \qquad \text{(B.5)}
\end{aligned}
$$

For positive-b angularities, the factor $((1-x)^{-b} + x^{-b})^{\frac{2\epsilon}{1+b}}$ yields a singular contribution as $x \to 0$, which we have factored out in the final step of eq. (B.5). This implies that for $b > 0$ the η-regulator is not required since the divergence due to $1/x^{1+\eta+\frac{2\epsilon\, b}{1+b}}$ as $x \to 0$ is already taken care of by the ϵ-regulator. Dropping the η-regulator, we expand the result for the unsubtracted jet diagram (b), for positive-b values, in powers of ϵ. The result, upon expansion, is given as

$$
\begin{aligned}
\mathcal{J}^{(1+)}_{b,\text{unsub}}(\tau_R, 0) = \frac{\alpha_s(\mu)\, C_F}{\pi} \Bigg[&\frac{1+b}{2\, b\, \epsilon^2}\, \delta(\tau_R) + \frac{1}{\epsilon}\delta(\tau_R) - \frac{1}{b\,\epsilon}\, \mathcal{L}^0\!\left(\frac{\tau_R}{m}\right) + \frac{2}{b(1+b)}\, \mathcal{L}_1\!\left(\frac{\tau_R}{m}\right) \\
&- \frac{2}{1+b}\, \mathcal{L}^0\!\left(\frac{\tau_R}{m}\right) - \frac{2}{1+b}\, \delta(\tau_R) \int_0^1 \mathrm{d}x\, \frac{(1-x)}{x} \ln\left(1 + \left(\frac{x}{1-x}\right)^b\right) + \frac{2\, b}{1+b}\, \delta(\tau_R) \\
&- \frac{\pi^2}{24}\, \frac{1+b}{b}\, \delta(\tau_R) + \mathcal{O}(\epsilon)\Bigg]. \qquad \text{(B.6)}
\end{aligned}
$$

This expression contains b-dependent ϵ-divergences which will cancel upon taking the appropriate zero-bin contribution into account.

JHEP08(2019)144

B.2.2 Negative-b angularities

As the test function, $((1-x)^{-b}+x^{-b})^{\frac{2\epsilon}{1+b}}$, is well defined for $b<0$, we rewrite the second line in eq. (B.5) for negative-b angularities as

$$\mathcal{J}^{(1-)}_{\text{b,unsub}}(\tau_R,0) = \frac{2}{1+b}\frac{\alpha_s(\mu)C_F}{\pi}\frac{e^{\epsilon\gamma_E}w^2}{\Gamma(1-\epsilon)}\left(\frac{\mu}{Q}\right)^{2\epsilon}\left(\frac{\nu}{Q}\right)^{\eta}\frac{1}{\tau_R^{1+\frac{2\epsilon}{1+b}}}\int_0^1 \mathrm{d}x\left(1+\left(\frac{x}{1-x}\right)^{-b}\right)^{\frac{2\epsilon}{1+b}} \times \frac{(1-x)^{1-\frac{2\epsilon\, b}{1+b}}}{x^{1+\eta}}\,, \tag{B.7}$$

to obtain the same form for the integral as in the positive-b case.

The result of the unsubtracted jet diagram (b), now requires the explicit use of the η-regulator to regularize the divergence as $x\to 0$. We expand the integrand in eq. (B.7) in η and ϵ ($\eta \ll \epsilon$) and perform the integral to obtain

$$\begin{aligned}\mathcal{J}^{(1-)}_{\text{b,naive}}(\tau_R,0) = \frac{\alpha_s(\mu)\,C_F}{\pi}\Bigg[&-\frac{2\,e^{\epsilon\gamma_E}w^2}{\eta\,(1+b)\,\Gamma(1-\epsilon)}\left(\frac{\mu}{Q}\right)^{2\epsilon}\mathcal{L}^{\frac{2\epsilon}{1+b}}(\tau_R;\infty)+\frac{1}{\epsilon}\,\delta(\tau_R)+\frac{1}{\epsilon}\ln\frac{\nu}{Q}\,\delta(\tau_R)\\ &-\frac{2}{1+b}\,\mathcal{L}^0\!\left(\frac{\tau_R}{m}\right)+\frac{2\,b}{1+b}\,\delta(\tau_R)-\frac{\pi^2\,b}{3(1+b)}\,\delta(\tau_R)-\frac{2}{1+b}\ln\frac{\nu}{Q}\,\mathcal{L}^0\!\left(\frac{\tau_R}{m}\right)\\ &-\frac{2}{1+b}\,\delta(\tau_R)\int_0^1\mathrm{d}x\,\frac{(1-x)}{x}\ln\!\left(1+\left(\frac{x}{1-x}\right)^{-b}\right)+\mathcal{O}(\eta,\epsilon)\Bigg]\,,\end{aligned} \tag{B.8}$$

where the full ϵ-dependence has been retained in the $1/\eta$-term according to the rapidity renormalization prescription [34].

B.3 Zero-bin contribution

The zero-bin subtraction to the jet diagram (b) can be evaluated by taking the gluon momentum to scale as $l^\mu \sim Q(\lambda^{1+b},\lambda^{1+b},\lambda^{1+b})$. This results to

$$\begin{aligned}\mathcal{J}^{(1\pm)}_{\text{b,0}}(\tau_R,0) &= 2\left(\frac{e^{\gamma_E}\mu^2}{4\pi}\right)^{\epsilon}\frac{(2\pi)^{3-2\epsilon}}{N_c}\int\frac{\mathrm{d}^d l}{(2\pi)^{d-1}}\delta(l^2)\,\theta(l^0)\int\frac{\mathrm{d}^d p}{(2\pi)^{d-1}}\delta(p^2)\,\theta(p^0)\,\delta(p^- - Q)\\ &\quad\times\delta\!\left(\tau_R-\frac{|\vec{p}_\perp|}{Q}\left(\frac{p^+}{p^-}\right)^{\frac{b}{2}}-\frac{|\vec{l}_\perp|}{Q}\left(\frac{l^+}{l^-}\right)^{\frac{b}{2}}\right)\delta^{d-2}(\vec{l}_\perp+\vec{p}_\perp)\,\mathrm{tr}\Bigg[\frac{\bar{\not{n}}}{2}\,\frac{i(\not{l}+\not{p})}{p^- l^+}\,(ig\,\gamma^\mu T^a)\\ &\quad\times u_s(p)\,\bar{u}_s(p)\,(-g_{\mu\nu})\,\frac{g\,\bar{n}^\nu T^a}{\bar{n}\cdot l}\Bigg]\\ &= \frac{2\alpha_s(\mu)C_F}{\pi}\frac{e^{\epsilon\gamma_E}}{\Gamma(1-\epsilon)}w^2\left(\frac{\nu}{Q}\right)^{\eta}\left(\frac{\mu}{Q}\right)^{2\epsilon}\frac{1}{1+b}\frac{1}{\tau_R^{1+\frac{2\epsilon}{1+b}}}\int_0^\infty\mathrm{d}x\,\frac{(1+x^{-b})^{\frac{2\epsilon}{1+b}}}{x^{1+\eta}}\\ &= \mathrm{sgn}(b)\frac{2\alpha_s(\mu)C_F}{\pi}\frac{e^{\epsilon\gamma_E}}{\Gamma(1-\epsilon)}w^2\left(\frac{\nu}{Q}\right)^{\eta}\left(\frac{\mu}{Q}\right)^{2\epsilon}\frac{1}{1+b}\frac{1}{\tau_R^{1+\frac{2\epsilon}{1+b}}}\frac{\Gamma(\frac{\eta}{b})\,\Gamma(-\frac{2\epsilon}{1+b}-\frac{\eta}{b})}{b\,\Gamma(-\frac{2\epsilon}{1+b})}\,,\end{aligned} \tag{B.9}$$

which holds for all $b>-1$. It is worth mentioning that the integral in the second line of the equation changes sign for negative-b angularities and hence we write the outcome as

JHEP08(2019)144

given in eq. (B.9). The final result, upon expansion in the regulators $\eta \ll \epsilon$ yields

$$\begin{aligned}\mathcal{J}^{(1\pm)}_{b,0}(\tau_R,0) = \frac{\alpha_s(\mu)\,C_F}{\pi}\mathrm{sgn}(b)\Bigg[&\frac{2\,w^2\,e^{\epsilon\,\gamma_E}}{\eta\,(1+b)\,\Gamma(1-\epsilon)}\left(\frac{\mu}{Q}\right)^{2\epsilon}\mathcal{L}^{\frac{2\epsilon}{1+b}}(\tau_R;\infty)\\ &+\frac{1+b}{2\,b\,\epsilon^2}\,\delta(\tau_R)-\frac{1}{b\,\epsilon}\,\mathcal{L}^0\!\left(\frac{\tau_R}{m}\right)-\frac{1}{\epsilon}\ln\frac{\nu}{Q}\,\delta(\tau_R)+\frac{2}{b(1+b)}\,\mathcal{L}_1\!\left(\frac{\tau_R}{m}\right)\\ &+\frac{2}{1+b}\,\ln\frac{\nu}{Q}\,\mathcal{L}^0\!\left(\frac{\tau_R}{m}\right)-\frac{\pi^2}{24\,b}\,\frac{b^2+2\,b+9}{1+b}\,\delta(\tau_R)+\mathcal{O}(\eta,\epsilon)\Bigg]\,. \end{aligned}\tag{B.10}$$

We stress that the zero-bin integral contains an η-divergence for all angularities. It is only the unsubtracted jet diagram (b) which does not require a rapidity regulator for $b > 0$ angularities.

C Evaluation of the one-loop soft function

Here we present the calculation of the soft function diagrams for all angularities ($b > -1$). The one-loop contribution to the soft function due to diagrams (a) and (b) of Figure 3, which give the same result due to symmetry, amounts to

$$\begin{aligned}&\mathcal{S}^{(1)}(\tau_L,\tau_R,\vec{p}_\perp^{\,2},\vec{k}_\perp^{\,2})\\ &=2\left(\frac{e^{\gamma_E}\mu^2}{4\pi}\right)^{\epsilon}\frac{\pi^{2-2\epsilon}\vec{k}_\perp^{-2\epsilon}\,\vec{p}_\perp^{-2\epsilon}}{N_c\,\Gamma^2(1-\epsilon)}\nu^\eta\,w^2\int\frac{\mathrm{d}^dl}{(2\pi)^{d-1}}\delta(l^2)\,\theta(l^0)|2\,l^3|^{-\eta}\Bigg\{\theta(l^3)\,\delta(\tau_L)\\ &\quad\delta\!\left(\tau_R-\frac{|\vec{l}_\perp|}{Q}\left(\frac{l^+}{l^-}\right)^{\frac{b}{2}}\right)\delta^{2-2\epsilon}(\vec{l}_\perp-\vec{p}_\perp)\,\delta^{2-2\epsilon}(\vec{k}_\perp)+\theta(-l^3)\,\delta\!\left(\tau_L-\frac{|\vec{l}_\perp|}{Q}\left(\frac{l^-}{l^+}\right)^{\frac{b}{2}}\right)\\ &\quad\delta(\tau_R)\,\delta^{2-2\epsilon}(\vec{l}_\perp-\vec{k}_\perp)\,\delta^{2-2\epsilon}(\vec{p}_\perp)\Bigg\}\mathrm{tr}\left[\frac{g\,n^\mu T^a}{l^+}\,\frac{g\,\bar{n}^\nu T^a}{-\,l^-}\right]\sum_{\mathrm{pol}}\epsilon^r_\mu(l)\,\epsilon^{*r}_\nu(l)\\ &=\frac{2\,\alpha_s(\mu)C_F}{\pi}e^{\epsilon\gamma_E}\mu^{2\epsilon}\frac{\vec{p}_\perp^{-2\epsilon}}{\Gamma(1-\epsilon)}\nu^\eta\,w^2\,\delta(\vec{k}_\perp^{\,2})\,\delta(\tau_L)\int\mathrm{d}^dl\;\delta(l^2)\,\theta(l^0)|2\,l^3|^{-\eta}\\ &\quad\left\{\theta(l^3)\,\delta\!\left(\tau_R-\frac{|\vec{l}_\perp|}{Q}\left(\frac{l^+}{l^-}\right)^{\frac{b}{2}}\right)\delta^{2-2\epsilon}(\vec{l}_\perp-\vec{p}_\perp)+\left\{\begin{array}{c}\tau_L\leftrightarrow\tau_R\\ \vec{k}_\perp^{\,2}\leftrightarrow\vec{p}_\perp^{\,2}\end{array}\right\}\right\}\frac{1}{l^+}\,\frac{1}{l^-}\\ &=\frac{\alpha_s(\mu)\,C_F}{\pi}\,\frac{\mu^{2\epsilon}e^{\epsilon\gamma_E}}{\Gamma(1-\epsilon)}\nu^\eta\,w^2\,Q\,\delta(\vec{k}_\perp^{\,2})\,\delta(\tau_L)\,\theta\!\left(\left(\frac{|\vec{p}_\perp|}{Q\,\tau_R}\right)^{1/b}-1\right)\\ &\quad\times(p_\perp^2)^{-1-\epsilon-\frac{\eta+1}{2}}\frac{\left|1-\left(\frac{Q\,\tau_R}{|\vec{p}_\perp|}\right)^{2/b}\right|^{-\eta}}{|b|\left(\frac{Q\,\tau_R}{|\vec{p}_\perp|}\right)^{1-\eta/b}}+\left\{\begin{array}{c}\tau_L\leftrightarrow\tau_R\\ \vec{k}_\perp^{\,2}\leftrightarrow\vec{p}_\perp^{\,2}\end{array}\right\}.\end{aligned}\tag{C.1}$$

As noted in the text, this expression contains coupled distribution in the variables τ_R and $p_\perp$ (or τ_L and $k_\perp$) which we decouple by making appropriate change of variables as shown in eqs. (4.3) and (4.10), respectively.

D Evaluation of the soft convolution integral

In this appendix, we calculate the soft convolution integrals $\mathrm{I}_s^{(+)}(\tau_R)$ and $\mathrm{I}_s^{(-)}(\tau_R)$ entering the cross sections for positive and negative values of b, respectively.

JHEP08(2019)144

D.1 Soft convolution integral $\mathrm{I}_s^{(+)}(\tau_R)$

The integral $\mathrm{I}_s^{(+)}(\tau_R)$ as defined in eq. (5.5), is given by

$$\mathrm{I}_s^{(+)}(\tau_R) \equiv \frac{2}{b}\int_0^{Q\,\tau_R^{1/(1+b)}} dp_\perp\,\theta\Big(\frac{p_\perp}{Q}-\tau_R+\Big(\frac{p_\perp}{Q}\Big)^{1+b}\Big)\frac{Q}{p_\perp}\,\frac{1}{\mu}\Big[\frac{1}{p_\perp/\mu}\Big]_+\Big[\frac{p_\perp/Q}{\tau_R-\Big(\frac{p_\perp}{Q}\Big)^{1+b}}\Big]_+ . \tag{D.1}$$

First of all, we perform a change of variables as

$$\Big(\frac{p_\perp}{Q}\Big)^{1+b}=\rho \quad \text{implying} \quad dp_\perp=\frac{Q}{1+b}\,\rho^{\frac{-b}{1+b}}\,d\rho\,. \tag{D.2}$$

Writing the integral in terms of dimensionless quantities ρ and τ_R gives

$$\begin{aligned}
\mathrm{I}_s^{(+)}(\tau_R) &= \frac{2}{b\,(1+b)}\int_0^{\tau_R} d\rho\,\theta(\rho+\rho^{\frac{1}{1+b}}-\tau_R)\frac{1}{\rho}\frac{Q}{\mu}\Big[\frac{\mu/Q}{\rho^{\frac{1}{1+b}}}\Big]_+\Big[\frac{\rho^{\frac{1}{1+b}}}{\tau_R-\rho}\Big]_+ \\
&= \frac{2}{b(1+b)}\int_0^{\tau_R} d\rho\,\theta(\rho+\rho^{\frac{1}{1+b}}-\tau_R)\frac{1}{\rho}\Big(\Big[\frac{1}{\rho^{\frac{1}{1+b}}}\Big]_+-(1+b)\ln\frac{\mu}{Q}\,\rho^{\frac{b}{1+b}}\delta(\rho)\Big)\Big[\frac{\rho^{\frac{1}{1+b}}}{\tau_R-\rho}\Big]_+ \\
&= \frac{2}{b\,(1+b)}\int_0^{\tau_R} d\rho\,\theta(\rho+\rho^{\frac{1}{1+b}}-\tau_R)\frac{1}{\rho}\Big[\frac{1}{\rho^{\frac{1}{1+b}}}\Big]_+\Big[\frac{\rho^{\frac{1}{1+b}}}{\tau_R-\rho}\Big]_+ .
\end{aligned} \tag{D.3}$$

In the second line of the above equation, the $\delta(\rho)$ term does not contribute. Using the following identities for the plus distributions appearing above,

$$\Big[\frac{\rho^{\frac{1}{1+b}}}{\tau-\rho}\Big]_+ = -\frac{\rho^{\frac{1}{1+b}}}{1+b}\ln\rho\,\delta(\rho-\tau)+\rho^{\frac{1}{1+b}}\Big[\frac{1}{\tau-\rho}\Big]_+ , \tag{D.4}$$

$$\frac{\rho^{\frac{1}{1+b}}}{\rho}\Big[\frac{1}{\rho^{\frac{1}{1+b}}}\Big]_+ = \Big[\frac{1}{\rho}\Big]_+ , \tag{D.5}$$

$$\frac{\rho^{\frac{1}{1+b}}\ln\rho}{\rho}\Big[\frac{1}{\rho^{\frac{1}{1+b}}}\Big]_+ = \Big[\frac{\ln\rho}{\rho}\Big]_+ , \tag{D.6}$$

Eq. (D.3) can be rewritten in the form

$$\begin{aligned}
\mathrm{I}_s^{(+)}(\tau_R) &= \frac{2}{b(1+b)}\int_0^{\tau_R} d\rho\,\theta(\rho+\rho^{\frac{1}{1+b}}-\tau_R)\frac{1}{\rho}\Big[\frac{1}{\rho^{\frac{1}{1+b}}}\Big]_+ \\
&\quad\times\Big(-\frac{\rho^{\frac{1}{1+b}}}{1+b}\ln\rho\,\delta(\rho-\tau_R)+\rho^{\frac{1}{1+b}}\Big[\frac{1}{\tau_R-\rho}\Big]_+\Big) \\
&= \frac{2}{b(1+b)}\Big(-\frac{1}{1+b}\Big[\frac{\ln\tau_R}{\tau_R}\Big]_+ + \int_{r\,\tau_R}^{\tau_R} d\rho\,\Big[\frac{1}{\rho}\Big]_+\Big[\frac{1}{\tau_R-\rho}\Big]_+\Big) .
\end{aligned} \tag{D.7}$$

Here the lower limit of integration corresponding to the Heaviside θ-function is determined by the solution of the equation

$$\frac{r}{(1-r)^{1+b}}=\tau_R^b\,. \tag{D.8}$$

JHEP08(2019)144

Eq. (D.7) has the familiar form of a convolution of two plus distributions except for the fact that the lower limit is now regulated by $r\,\tau_R$. This lower cut-off regulates the singularity due to $1/\rho$ as $\rho \to 0$, thereby allowing us to drop the first plus prescription in the last line of eq. (D.7). The other singular limit for $\rho \to \tau_R$ can be regulated explicitly by raising the second term in the convolution to the power of $1+\alpha$. The final result, which is obtained by extracting the α^0-terms of this regulated integral, gives

$$\mathrm{I}_s^{(+)}(\tau_R) = -\frac{2\,b}{(1+b)^2}\left[\frac{\ln\tau_R}{\tau_R}\right]_+ - \frac{\pi^2}{3\,b(1+b)}\delta(\tau_R) - \frac{2}{1+b}\frac{\ln(1-r)}{\tau_R}\,. \tag{D.9}$$

D.2 Soft convolution integral $\mathrm{I}_s^{(-)}(\tau_R)$

The integral $\mathrm{I}_s^{(-)}(\tau_R)$ as defined in eq. (5.24), is given by

$$\begin{aligned}\mathrm{I}_s^{(-)}(\tau_R) &\equiv -\frac{2}{b(1+b)}\int_{s\,\tau_R}^{\tau_R}\mathrm{d}\tau_n^s\,\frac{1}{(\tau_n^s)^2}\frac{1}{(\tau_R-\tau_n^s)^{\frac{b-1}{1+b}}}\left[\frac{(\tau_n^s)^2}{(\tau_R-\tau_n^s)^{\frac{2}{1+b}}}\right]_+\frac{Q}{\mu}\left[\frac{1}{Q\tau_n^s/\mu}\right]_+ \\ &= -\frac{2}{b(1+b)}\left(-(1+b)\left[\frac{\ln\tau_R}{\tau_R}\right]_+ + \int_{s\,\tau_R}^{\tau_R}\mathrm{d}\tau_n^s\left[\frac{1}{\tau_R-\tau_n^s}\right]_+\left[\frac{1}{\tau_R}\right]_+\right).\end{aligned} \tag{D.10}$$

Here again the lower limit of integration is given by the solution of a transcendental equation,

$$\frac{s}{(1-s)^{\frac{1}{1+b}}} = \tau_R^{-\frac{b}{1+b}}\,. \tag{D.11}$$

Eq. (D.10) has the form of a convolution of plus distributions but with a modified lower limit. This convolution integral can be calculated in a similar way as outlined for the positive-b case, leading to

$$\mathrm{I}_s^{(-)}(\tau_R) = \frac{2\,b}{(1+b)^2}\left[\frac{\ln\tau_R}{\tau_R}\right]_+ + \frac{\pi^2}{3\,b(1+b)}\delta(\tau_R) - \frac{2}{(1+b)^2}\frac{\ln(1-s)}{\tau_R}\,. \tag{D.12}$$

E Expansion of the constraint equations in various limits

Here we discuss the appropriate expansions for the constraint eqs. (D.8) and (D.11) in various limits.

E.1 Solution to the constraint equation in r ($b > 0$)

We start with positive values of the angularity exponent, and treat separately the case of vanishingly small b.

E.1.1 Small-τ expansion for r

In the small-τ limit, the lowest-order solution to eq. (D.8) goes like τ_R^b. The general solution can then be written as a series in τ_R^b,

$$r = a_1\tau_R^b + a_2\tau_R^{2\,b} + a_3\tau_R^{3\,b} + a_4\tau_R^{4\,b} + a_5\tau_R^{5\,b} + \dots\,, \tag{E.1}$$

JHEP08(2019)144

where

$$a_1 = 1, \quad a_2 = -(1+b), \quad a_3 = \frac{3\,b^2}{2} + \frac{5\,b}{2} + 1, \quad a_4 = -\frac{8\,b^3}{3} - 6\,b^2 - \frac{13\,b}{3} - 1$$
$$a_5 = \frac{125\,b^4}{24} + \frac{175\,b^3}{12} + \frac{355\,b^2}{24} + \frac{77\,b}{12} + 1, \quad \dots\,. \tag{E.2}$$

The $\ln(1-r)/\tau_R$ term in eq. (5.9) is well-defined for $r \sim \tau_R^b$ and does not require any plus prescription since a finite value of b regulates the limit $\tau_R \to 0$. Eq. (5.9), in this limit, can then be written as

$$\begin{aligned}\mathrm{I}_s^{(+)}(\tau_R) &= -\frac{2\,b}{(1+b)^2}\left[\frac{\ln\tau_R}{\tau_R}\right]_+ - \frac{\pi^2}{3\,b(1+b)}\delta(\tau_R) - \frac{2}{1+b}\frac{\ln(1-a_1\tau_R^b - a_2\tau_R^{2\,b} - a_3\tau_R^{3\,b} + \dots)}{\tau_R} \\ &= -\frac{2\,b}{(1+b)^2}\left[\frac{\ln\tau_R}{\tau_R}\right]_+ - \frac{\pi^2}{3\,b(1+b)}\delta(\tau_R) - \frac{2}{1+b}\sum_{n=1}^{\infty}\frac{c_n}{\tau_R^{1-n\,b}}\,,\end{aligned} \tag{E.3}$$

with coefficients c_n given in eq. (5.13). The last term accounts for sub-leading singular contributions and/or power corrections depending on the value of b.

E.1.2 Small-b expansion for r

Any truncation of the power series expansion in eq. (E.1) ceases to provide the correct solution to eq. (D.8) when τ and b are both close to zero such that $\tau_R^b \sim 1$. In this case, the general solution can instead be represented as an expansion in powers of b,

$$r = r_0 + b\,r_1 + b^2\,r_2 + \dots\,, \tag{E.4}$$

where the leading-order solution r_0 is determined by

$$\frac{r_0}{1-r_0} = \tau_R^b\,. \tag{E.5}$$

Using the last equation and the power series expansion in eq. (E.4), the coefficients r_1, r_2, $\dots$ can be obtained from eq. (D.8) as

$$\begin{aligned} r_0 &= \frac{\tau_R^b}{1+\tau_R^b}, \qquad r_1 = -\frac{\tau_R^b\ln(1+\tau_R^b)}{(1+\tau_R^b)^2}, \\ r_2 &= -\frac{\tau_R^b\Big((\tau_R^b-1)\ln(1+\tau_R^b) - 2\,\tau_R^b\Big)\ln(1+\tau_R^b)}{2\,(1+\tau_R^b)^3} \qquad \dots\,. \end{aligned} \tag{E.6}$$

Note that the leading-order solution r_0 in this case has a well-defined limit, i.e. as b becomes vanishingly small, r_0 converges to $1/2$ as expected.

Finally, to obtain the small-b limit of the soft convolution integral of eq. (5.9), we need to take the small-b limit of $\ln(1-r)/\tau_R$. Since b regulates small-τ_R limit, $\ln(1-r)/\tau_R$ becomes a distribution in τ_R. We get,

$$\frac{\ln(1-r)}{\tau_R} = \left(-\frac{\pi^2}{12\,b} + \frac{\ln^2 2}{2} - \frac{b\ln^2 2}{4}\right)\delta(\tau_R) - \ln 2\left[\frac{1}{\tau_R}\right]_+ - \frac{b}{2}\left[\frac{\ln\tau_R}{\tau_R}\right]_+ + \frac{b\ln 2}{2}\left[\frac{1}{\tau_R}\right]_+ + \mathcal{O}(b^2)\,. \tag{E.7}$$

JHEP08(2019)144

This finally gives

$$\mathrm{I}_s^{(+)}(\tau_R) = \delta(\tau_R)\left(-\frac{\pi^2}{6\,b} + \frac{\pi^2}{6} - \frac{\pi^2\,b}{6} - \ln^2 2 + \frac{3\,b}{2}\,\ln^2 2\right) + 2\ln 2\left[\frac{1}{\tau_R}\right]_+ - 3\,b\ln 2\left[\frac{1}{\tau_R}\right]_+ - b\left[\frac{\ln\tau_R}{\tau_R}\right]_+ + \mathcal{O}(b^2)\,. \tag{E.8}$$

E.2 Solution to the constraint equation in s ($b < 0$)

Analogously, we now treat the case of negative angularity exponents.

E.2.1 Small-τ expansion for s

In the small-τ limit, eq. (D.11) admits a solution of the form

$$s = a_1^{'}\tau_R^{-\frac{b}{1+b}} + a_2^{'}\tau_R^{-\frac{2\,b}{1+b}} + a_3^{'}\tau_R^{-\frac{3\,b}{1+b}} + a_4^{'}\tau_R^{-\frac{4\,b}{1+b}} + a_5^{'}\tau_R^{-\frac{5\,b}{1+b}} + \dots\,, \tag{E.9}$$

where the first few coefficients $a_n^{'}$ are given by

$$a_1^{'} = 1, \quad a_2^{'} = -\frac{1}{1+b}, \quad a_3^{'} = -\frac{b-2}{2(1+b)^2}, \quad a_4^{'} = -\frac{b^2-4\,b+3}{3(1+b)^3}$$
$$a_5^{'} = -\frac{6\,b^3 - 37\,b^2 + 58\,b - 24}{24(1+b)^4}, \quad \dots\,. \tag{E.10}$$

The last term in eq. (D.12) is well-defined in this limit and does not require any plus prescription, as earlier. The soft convolution integral in eq. (D.12) can be written as

$$\begin{aligned}\mathrm{I}_s^{(-)}(\tau_R) &= \frac{2\,b}{(1+b)^2}\left[\frac{\ln\tau_R}{\tau_R}\right]_+ + \frac{\pi^2}{3\,b(1+b)}\delta(\tau_R) - \frac{2}{(1+b)^2}\frac{\ln\left(1 - a_1^{'}\tau_R^{-\frac{b}{1+b}} - a_2^{'}\tau_R^{-\frac{2\,b}{1+b}} + \dots\right)}{\tau_R} \\ &= \frac{2\,b}{(1+b)^2}\left[\frac{\ln\tau_R}{\tau_R}\right]_+ + \frac{\pi^2}{3\,b(1+b)}\delta(\tau_R) - \frac{2}{(1+b)^2}\sum_{n=1}^{\infty}\frac{c_n^{'}}{\tau_R^{1+\frac{n\,b}{1+b}}}\,.\end{aligned} \tag{E.11}$$

with coefficients $c_n^{'}$ given in eq. (5.29). Notice that for a given negative value of b, only the terms with $N = max(n) < \lceil 1/|b| \rceil - 1$ in the summation are singular. Thus for $-1 < b < -0.5$, the extra terms amount only to power corrections and there is no sub-leading singular contribution from recoil.

E.2.2 Small-b expansion for s

The solution in eq. (E.9) cannot be applied when b and τ are both vanishingly small. In this limit, a general solution to the constraint equation can be written, similar to eq. (E.4), as

$$s = s_0 + b\,s_1 + b^2\,s_2 + \dots\,, \tag{E.12}$$

with the leading-order solution s_0 determined by

$$\frac{s_0}{1-s_0} = \tau_R^{-b}\,. \tag{E.13}$$

JHEP08(2019)144

The first few coefficients of the series expansion in eq. (E.12) are

$$s_0 = \frac{\tau_R^{-b}}{1+\tau_R^{-b}}, \qquad s_1 = -\frac{\tau_R^{-b}\ln\left(\frac{\tau_R^{-b}}{1+\tau_R^{-b}}\right)}{(1+\tau_R^{-b})^2},$$
$$s_2 = \frac{\tau_R^{-b}\ln\left(\frac{\tau_R^{-b}}{1+\tau_R^{-b}}\right)\left(2-(\tau_R^{-b}-1)\ln\left(\frac{\tau_R^{-b}}{1+\tau_R^{-b}}\right)\right)}{2\,(1+\tau_R^{-b})^3} \qquad \ldots\,. \tag{E.14}$$

Upon expansion in b, the term $\ln(1-s)/\tau_R$ in the soft convolution integral becomes a distribution in τ, as follows

$$\frac{\ln(1-s)}{\tau_R} = \left(\frac{\pi^2}{12\,b}+\frac{\pi^2}{12}+\frac{\ln^2 2}{2}+\frac{b}{4}\ln^2 2\right)\delta(\tau_R) - \ln 2\left[\frac{1}{\tau_R}\right]_+ + \frac{b}{2}\left[\frac{\ln\tau_R}{\tau_R}\right]_+ - \frac{b}{2}\ln 2\left[\frac{1}{\tau_R}\right]_+ + \mathcal{O}(b^2)\,, \tag{E.15}$$

which leads to the following result in the small-τ and small-b limit,

$$\mathrm{I}_s^{(-)}(\tau_R) = \delta(\tau_R)\left(\frac{\pi^2}{6\,b}-\frac{\pi^2}{6}+\frac{\pi^2\,b}{6}-\ln^2 2+\frac{3\,b}{2}\ln^2 2\right) + 2\ln 2\left[\frac{1}{\tau_R}\right]_+ - 3\,b\ln 2\left[\frac{1}{\tau_R}\right]_+ + b\left[\frac{\ln\tau_R}{\tau_R}\right]_+ + \mathcal{O}(b^2)\,. \tag{E.16}$$

Open Access. This article is distributed under the terms of the Creative Commons Attribution License (CC-BY 4.0), which permits any use, distribution and reproduction in any medium, provided the original author(s) and source are credited.

References

[1] M. Dasgupta and G.P. Salam, *Event shapes in e^+e^- annihilation and deep inelastic scattering*, *J. Phys.* **G 30** (2004) R143 [hep-ph/0312283] [INSPIRE].

[2] T. Becher and M.D. Schwartz, *A precise determination of α_s from LEP thrust data using effective field theory*, *JHEP* **07** (2008) 034 [arXiv:0803.0342] [INSPIRE].

[3] R.A. Davison and B.R. Webber, *Non-Perturbative Contribution to the Thrust Distribution in e^+e^- Annihilation*, *Eur. Phys. J.* **C 59** (2009) 13 [arXiv:0809.3326] [INSPIRE].

[4] R. Abbate, M. Fickinger, A.H. Hoang, V. Mateu and I.W. Stewart, *Thrust at N^3LL with Power Corrections and a Precision Global Fit for $\alpha_s(m_Z)$*, *Phys. Rev.* **D 83** (2011) 074021 [arXiv:1006.3080] [INSPIRE].

[5] T. Gehrmann, G. Luisoni and P.F. Monni, *Power corrections in the dispersive model for a determination of the strong coupling constant from the thrust distribution*, *Eur. Phys. J.* **C 73** (2013) 2265 [arXiv:1210.6945] [INSPIRE].

[6] A.H. Hoang, D.W. Kolodrubetz, V. Mateu and I.W. Stewart, *Precise determination of α_s from the C-parameter distribution*, *Phys. Rev.* **D 91** (2015) 094018 [arXiv:1501.04111] [INSPIRE].

[7] A. Banfi, G.P. Salam and G. Zanderighi, *Resummed event shapes at hadron-hadron colliders*, *JHEP* **08** (2004) 062 [hep-ph/0407287] [INSPIRE].

JHEP08(2019)144

[8] A. Banfi, G.P. Salam and G. Zanderighi, *Phenomenology of event shapes at hadron colliders*, *JHEP* **06** (2010) 038 [arXiv:1001.4082] [INSPIRE].

[9] A. Banfi, G. Marchesini and G. Smye, *Away from jet energy flow*, *JHEP* **08** (2002) 006 [hep-ph/0206076] [INSPIRE].

[10] M. Dasgupta and G.P. Salam, *Resummation of nonglobal QCD observables*, *Phys. Lett.* **B 512** (2001) 323 [hep-ph/0104277] [INSPIRE].

[11] A. Hornig, Y. Makris and T. Mehen, *Jet Shapes in Dijet Events at the LHC in SCET*, *JHEP* **04** (2016) 097 [arXiv:1601.01319] [INSPIRE].

[12] A.J. Larkoski, I. Moult and B. Nachman, *Jet Substructure at the Large Hadron Collider: A Review of Recent Advances in Theory and Machine Learning*, arXiv:1709.04464 [INSPIRE].

[13] C.F. Berger, T. Kucs and G.F. Sterman, *Event shape/energy flow correlations*, *Phys. Rev.* **D 68** (2003) 014012 [hep-ph/0303051] [INSPIRE].

[14] C.F. Berger and L. Magnea, *Scaling of power corrections for angularities from dressed gluon exponentiation*, *Phys. Rev.* **D 70** (2004) 094010 [hep-ph/0407024] [INSPIRE].

[15] A. Hornig, C. Lee and G. Ovanesyan, *Effective Predictions of Event Shapes: Factorized, Resummed and Gapped Angularity Distributions*, *JHEP* **05** (2009) 122 [arXiv:0901.3780] [INSPIRE].

[16] S.D. Ellis, C.K. Vermilion, J.R. Walsh, A. Hornig and C. Lee, *Jet Shapes and Jet Algorithms in SCET*, *JHEP* **11** (2010) 101 [arXiv:1001.0014] [INSPIRE].

[17] P. Achard et al., *Generalized event shape and energy flow studies in e^+e^- annihilation at $\sqrt{s} = 91.2\,GeV$–208.0-GeV*, *JHEP* **10** (2011) 143 [INSPIRE].

[18] E. Farhi, *A QCD Test for Jets*, *Phys. Rev. Lett.* **39** (1977) 1587 [INSPIRE].

[19] S. Brandt, C. Peyrou, R. Sosnowski and A. Wroblewski, *The Principal axis of jets. An Attempt to analyze high-energy collisions as two-body processes*, *Phys. Lett.* **12** (1964) 57 [INSPIRE].

[20] P.E.L. Rakow and B.R. Webber, *Transverse Momentum Moments of Hadron Distributions in QCD Jets*, *Nucl. Phys.* **B 191** (1981) 63 [INSPIRE].

[21] S. Catani, G. Turnock and B.R. Webber, *Jet broadening measures in e^+e^- annihilation*, *Phys. Lett.* **B 295** (1992) 269 [INSPIRE].

[22] G. Bell, A. Hornig, C. Lee and J. Talbert, *e^+e^- angularity distributions at NNLL′ accuracy*, *JHEP* **01** (2019) 147 [arXiv:1808.07867] [INSPIRE].

[23] Y.L. Dokshitzer, A. Lucenti, G. Marchesini and G.P. Salam, *On the QCD analysis of jet broadening*, *JHEP* **01** (1998) 011 [hep-ph/9801324] [INSPIRE].

[24] A.J. Larkoski, D. Neill and J. Thaler, *Jet Shapes with the Broadening Axis*, *JHEP* **04** (2014) 017 [arXiv:1401.2158] [INSPIRE].

[25] M. Procura, W.J. Waalewijn and L. Zeune, *Joint resummation of two angularities at next-to-next-to-leading logarithmic order*, *JHEP* **10** (2018) 098 [arXiv:1806.10622] [INSPIRE].

[26] A. Banfi, B.K. El-Menoufi and P.F. Monni, *The Sudakov radiator for jet observables and the soft physical coupling*, [arXiv:1807.11487] [INSPIRE].

JHEP08(2019)144

[27] C.W. Bauer, S. Fleming and M.E. Luke, *Summing Sudakov logarithms in $B \to X(s\gamma)$ in effective field theory*, Phys. Rev. **D 63** (2000) 014006 [hep-ph/0005275] [INSPIRE].

[28] C.W. Bauer, S. Fleming, D. Pirjol and I.W. Stewart, *An Effective field theory for collinear and soft gluons: Heavy to light decays*, Phys. Rev. **D 63** (2001) 114020 [hep-ph/0011336] [INSPIRE].

[29] C.W. Bauer and I.W. Stewart, *Invariant operators in collinear effective theory*, Phys. Lett. **B 516** (2001) 134 [hep-ph/0107001] [INSPIRE].

[30] C.W. Bauer, D. Pirjol and I.W. Stewart, *Soft collinear factorization in effective field theory*, Phys. Rev. **D 65** (2002) 054022 [hep-ph/0109045] [INSPIRE].

[31] C.W. Bauer, S. Fleming, D. Pirjol, I.Z. Rothstein and I.W. Stewart, *Hard scattering factorization from effective field theory*, Phys. Rev. **D 66** (2002) 014017 [hep-ph/0202088] [INSPIRE].

[32] A. Budhraja, A. Jain and M. Procura, *NLL resummation of recoil-sensitive angularities using SCET*, in preparation.

[33] C.F. Berger and G.F. Sterman, *Scaling rule for nonperturbative radiation in a class of event shapes*, JHEP **09** (2003) 058 [hep-ph/0307394] [INSPIRE].

[34] J.-Y. Chiu, A. Jain, D. Neill and I.Z. Rothstein, *A Formalism for the Systematic Treatment of Rapidity Logarithms in Quantum Field Theory*, JHEP **05** (2012) 084 [arXiv:1202.0814] [INSPIRE].

[35] L.G. Almeida, S.D. Ellis, C. Lee, G. Sterman, I. Sung and J.R. Walsh, *Comparing and counting logs in direct and effective methods of QCD resummation*, JHEP **04** (2014) 174 [arXiv:1401.4460] [INSPIRE].

[36] A.H. Hoang, D.W. Kolodrubetz, V. Mateu and I.W. Stewart, *C-parameter distribution at N^3LL' including power corrections*, Phys. Rev. **D 91** (2015) 094017 [arXiv:1411.6633] [INSPIRE].

[37] A. Banfi, H. McAslan, P.F. Monni and G. Zanderighi, *A general method for the resummation of event-shape distributions in e^+e^- annihilation*, JHEP **05** (2015) 102 [arXiv:1412.2126] [INSPIRE].

[38] T. Becher and G. Bell, *NNLL Resummation for Jet Broadening*, JHEP **11** (2012) 126 [arXiv:1210.0580] [INSPIRE].

[39] G.P. Salam and D. Wicke, *Hadron masses and power corrections to event shapes*, JHEP **05** (2001) 061 [hep-ph/0102343] [INSPIRE].

[40] V. Mateu, I.W. Stewart and J. Thaler, *Power Corrections to Event Shapes with Mass-Dependent Operators*, Phys. Rev. **D 87** (2013) 014025 [arXiv:1209.3781] [INSPIRE].

[41] J.-y. Chiu, A. Jain, D. Neill and I.Z. Rothstein, *The Rapidity Renormalization Group*, Phys. Rev. Lett. **108** (2012) 151601 [arXiv:1104.0881] [INSPIRE].

[42] T. Becher, G. Bell and M. Neubert, *Factorization and Resummation for Jet Broadening*, Phys. Lett. **B 704** (2011) 276 [arXiv:1104.4108] [INSPIRE].

[43] A. Idilbi and I. Scimemi, *Singular and Regular Gauges in Soft Collinear Effective Theory: The Introduction of the New Wilson Line T*, Phys. Lett. **B 695** (2011) 463 [arXiv:1009.2776] [INSPIRE].

JHEP08(2019)144

[44] A.V. Manohar, *Deep inelastic scattering as $x \to 1$ using soft collinear effective theory*, *Phys. Rev.* **D 68** (2003) 114019 [hep-ph/0309176] [INSPIRE].

[45] C.W. Bauer, C. Lee, A.V. Manohar and M.B. Wise, *Enhanced nonperturbative effects in Z decays to hadrons*, *Phys. Rev.* **D 70** (2004) 034014 [hep-ph/0309278] [INSPIRE].

[46] M.D. Schwartz, *Resummation and NLO matching of event shapes with effective field theory*, *Phys. Rev.* **D 77** (2008) 014026 [arXiv:0709.2709] [INSPIRE].

[47] A.V. Manohar and I.W. Stewart, *The Zero-Bin and Mode Factorization in Quantum Field Theory*, *Phys. Rev.* **D 76** (2007) 074002 [hep-ph/0605001] [INSPIRE].

[48] M.D. Schwartz, *Quantum Field Theory and the Standard Model*, Cambridge University Press, Cambridge U.K. (2014).

[49] S. Catani and M.H. Seymour, *A General algorithm for calculating jet cross-sections in NLO QCD*, *Nucl. Phys.* **B 485** (1997) 291 [*Erratum ibid.* **B 510** (1998) 503] [hep-ph/9605323] [INSPIRE].

JHEP08(2019)144